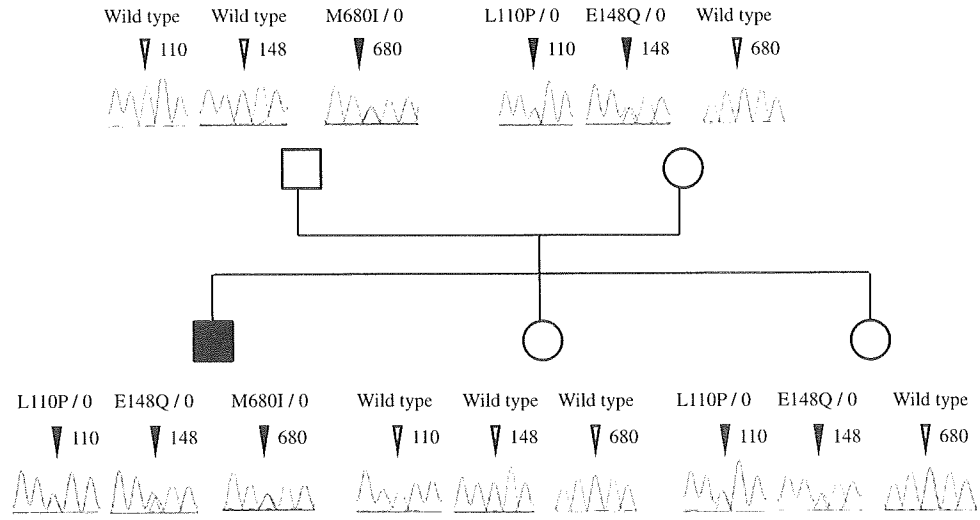

Fig. 1 Pedigree and chromatograms of the *MEFV* gene at amino acid positions 110, 148, and 680. *Black arrowheads* show heterozygous mutations for L110P, E148Q or M680I

None of his family members had these symptoms. From the age of 6 years, he experienced these symptoms about once every 2 months. At the time of the fever attack, he could not breathe deeply due to the chest pain. Subsequently rapid shallow breathing was recognized. Laboratory examinations showed mild leucocytosis (13,200 WBCs/μl) and elevated levels of C-reactive protein (CRP) (5.9 mg/dl) during an episode. Chest X-ray and electrocardiography revealed no abnormalities, and the patient did not have arthritis or rashes. Because he met the criteria for FMF based upon the Tel Hashomer criteria [2], we made a clinical diagnosis of FMF. After obtaining informed consent, we performed a genomic search for *MEFV*. Since the patient was found to be heterozygous for L110P–E148Q/M680I (Fig. 1), FMF was confirmed by the mutation in the hot spot of *MEFV*. The episodes were successfully prevented by administration of colchicine (0.25 mg/day).

Identification of M680I

After informed consent was obtained, the DNA of the patient, his parents, and 2 sisters was extracted from their peripheral blood mononuclear cells. The coding exons and flanking intronic sequences of the *MEFV* gene were amplified by polymerase chain reaction (PCR). The sequences of the PCR primers are available on request. The PCR products were treated using an ExoSAP-IT kit (GE Healthcare, Amersham, UK), and then analyzed by direct sequencing with an ABI 3130 DNA sequencer (Perkin-Elmer, Foster City, CA).

The results of the analysis are shown in Fig. 1. The L110P, E148Q, and M680I mutations were found in the patient. The patient's father was heterozygous only for the M680I mutation, and his mother carried the L110P and E148Q mutations. On the basis of the mutations carried by the parents, the patient was found to be heterozygous for L110P–E148Q/M680I. These mutations were not detected in his one sister, and his younger sister was heterozygous for L110P–E148Q. Interestingly, his mother and elder sister were heterozygous for the G304R mutation, which cause exon 2 skipping in pyrin (data not shown).

Discussion

Recently, a meta-analysis study on the founder populations (Jews, Armenians, Arabs, and Turks) for *MEFV* mutations revealed that the most frequent mutations detected in FMF patients are M694V (39.6%), V726A (13.9%), M680I (11.4%), E148Q (3.4%), and M694I (2.9%) [9]. The 4 major disease-causing mutations (M694V, M694I, M680I, and V726A) in exon 10 of *MEFV* have low allele frequencies in normal Japanese individuals [13]. Even for M694I, which seems to be the most common mutation in Japanese FMF patients [15], allele frequency was below 0.001 [13]. We recently reported that the common *MEFV* mutation patterns were E148Q/M694I (25.0%), L110P–E148Q/M694I (17.5%), and M694I alone (17.5%), and that the M694V, M680I or V726A mutations were not found in 80 Japanese FMF patients [15]. Some reports indicate that homozygous or compound heterozygous M680I mutations are associated with a moderate phenotype of the disease [16, 17]. Moreover, previous reports indicate that the M680I mutation, commonly seen in Armenians, is associated with a milder phenotype of the disease and lower frequency of amyloidosis [18, 19]. On the other hand, FMF patient heterozygous for the M680I gene mutation was reported to have developed nephritic syndrome [20]. Although we did not find abnormalities in chest imaging findings at the time of the fever attack, we strongly suspected presence of thoracic serositis because chest pain

accompanied by rapid shallow breathing are typical concomitant symptoms of FMF. Our patient is the first with the M680I mutation in Japan, and he showed comparatively mild clinical symptoms.

The patient's mother and one sister were found to be heterozygous for the G304R mutation, which causes exon 2 skipping in pyrin. There is no report that this mutation causes FMF [7], and the relationship between L110P–E148Q/M680I and G304R in this family remains unclear. Although the *MEFV* mutations E148Q and M694I are common in Japan, our finding shows that FMF associated with the M680I mutation certainly exists in the Japanese population.

Conflict of interest statement None.

References

1. Sohar E, Gafni J, Pras M, Heller H. Familial Mediterranean fever. A survey of 470 cases and review of the literature. Am J Med. 1967;43(2):227–53.
2. Livneh A, Langevitz P, Zemer D, Zaks N, Kees S, Lidar T, et al. Criteria for the diagnosis of familial Mediterranean fever. Arthritis Rheum. 1997;40(10):1879–85.
3. Ben-Chetrit E, Levy M. Familial Mediterranean fever. Lancet. 1998;351(9103):659–64.
4. Ancient missense mutations in a new member of the RoRet gene family are likely to cause familial Mediterranean fever. The International FMF Consortium. Cell. 1997;90(4):797–807.
5. French FMFC. A candidate gene for familial Mediterranean fever. Nat Genet. 1997;17(1):25–31.
6. Bernot A, da Silva C, Petit JL, Cruaud C, Caloustian C, Castet V, et al. Non-founder mutations in the MEFV gene establish this gene as the cause of familial Mediterranean fever (FMF). Hum Mol Genet. 1998;7(8):1317–25.
7. Infevers. The registry of Familial Mediterranean Fever (FMF) and hereditary auto-inflammatory disorders mutations. http://fmf.igh.cnrs.fr/ISSAID/infevers/ (2009).
8. Booth DR, Gillmore JD, Booth SE, Pepys MB, Hawkins PN. Pyrin/marenostrin mutations in familial Mediterranean fever. QJM. 1998;91(9):603–6.
9. Papadopoulos VP, Giaglis S, Mitroulis I, Ritis K. The population genetics of familial mediterranean fever: a meta-analysis study. Ann Hum Genet. 2008;72(Pt 6):752–61.
10. Touitou I. Standardized testing for mutations in familial Mediterranean fever. Clin Chem. 2003;49(11):1781–2.
11. Inal A, Yilmaz M, Kendirli SG, Altintas DU, Karakoc GB. The clinical and genetical features of 124 children with Familial Mediterranean fever: experience of a single tertiary center. Rheumatol Int. 2008;29(11):1279–85.
12. Majeed HA, El-Shanti H, Al-Khateeb MS, Rabaiha ZA. Genotype/phenotype correlations in Arab patients with familial Mediterranean fever. Semin Arthritis Rheum. 2002;31(6):371–6.
13. Sugiura T, Kawaguchi Y, Fujikawa S, Hirano Y, Igarashi T, Kawamoto M, et al. Familial Mediterranean fever in three Japanese patients, and a comparison of the frequency of MEFV gene mutations in Japanese and Mediterranean populations. Mod Rheumatol. 2008;18(1):57–9.
14. Tomiyama N, Higashiuesato Y, Oda T, Baba E, Harada M, Azuma M, et al. MEFV mutation analysis of familial Mediterranean fever in Japan. Clin Exp Rheumatol. 2008;26(1):13–7.
15. Tsuchiya-Suzuki A, Yazaki M, Nakamura A, Yamazaki K, Agematsu K, Matsuda M, et al. Clinical and Genetic Features of Familial Mediterranean Fever in Japan. J Rheumatol. 2009; 36(8):1671–6.
16. Gershoni-Baruch R, Brik R, Shinawi M, Livneh A. The differential contribution of MEFV mutant alleles to the clinical profile of familial Mediterranean fever. Eur J Hum Genet. 2002; 10(2):145–9.
17. Yalcinkaya F, Cakar N, Misirlioglu M, Tumer N, Akar N, Tekin M, et al. Genotype-phenotype correlation in a large group of Turkish patients with familial Mediterranean fever: evidence for mutation-independent amyloidosis. Rheumatology (Oxford). 2000;39(1):67–72.
18. Pras M. Familial Mediterranean fever: from the clinical syndrome to the cloning of the pyrin gene. Scand J Rheumatol. 1998;27(2):92–7.
19. Schwabe AD, Peters RS. Familial Mediterranean fever in Armenians. Analysis of 100 cases. Medicine (Baltimore). 1974;53(6):453–62.
20. Fisher PW, Ho LT, Goldschmidt R, Semerdjian RJ, Rutecki GW. Familial Mediterranean fever, inflammation and nephrotic syndrome: fibrillary glomerulopathy and the M680I missense mutation. BMC Nephrol. 2003;4:6.

Cytokine 47 (2009) 91–97

Contents lists available at ScienceDirect

Cytokine

journal homepage: www.elsevier.com/locate/issn/10434666

Interleukin-6 inhibits early differentiation of ATDC5 chondrogenic progenitor cells

Shoko Nakajima *, Takuya Naruto, Takako Miyamae, Tomoyuki Imagawa, Masaaki Mori, Shigeru Nishimaki, Shumpei Yokota

Department of Pediatrics, Yokohama City University School of Medicine, 3-9 Fukuura, Kanazawa-ku, Yokohama, Kanagawa 236-0004, Japan

ARTICLE INFO

Article history:
Received 18 February 2009
Received in revised form 25 April 2009
Accepted 7 May 2009

Keywords:
Interleukin-6
Anti-interleukin-6 receptor antibody
ATDC5
Chondrogenesis

ABSTRACT

Interleukin (IL)-6 is a causative agent of systemic juvenile idiopathic arthritis (sJIA), a chronic inflammatory disease complicated with severe growth impairment. Recent trials of anti-IL-6 receptor monoclonal antibody, tocilizumab, indicated that tocilizumab blocks IL-6/IL-6 receptor-mediated inflammation, and induces catch-up growth in children with sJIA. This study evaluates the effects of IL-6 on chondrogenesis by ATDC5 cells, a clonal murine chondrogenic cell line that provides an excellent model for studying endochondral ossification at growth plate. ATDC5 cells were examined for the expression of IL-6 receptor and gp130 by fluorescence-activated cell sorting analysis. Recombinant murine IL-6 was added to ATDC5 cultures to observe cell differentiation, using a quantitative RT-PCR for the chondrogenic differentiation markers type II collagen, aggrecan, and type X collagen. To block IL-6, the anti-mouse IL-6 receptor monoclonal antibody MR16-1 was added. As a result, the cells expressed IL-6 receptor and gp130. The expression of chondrogenic differentiation marker gene was reduced by IL-6, but this was abrogated by MR16-1. We conclude that IL-6 inhibits early chondrogenesis of ATDC5 cells suggesting that IL-6 may affect committed stem cells at a cellular level during chondrogenic differentiation of growth plate chondrocytes, and that IL-6 may be a cellular-level factor in growth impairment in sJIA.

1. Introduction

Longitudinal bone growth occurs at the growth plates, located at the ends of the long bones, by endochondral ossification, a two-step process in which cartilage is first formed and then remodeled into bone. Firstly, mesenchymal cells differentiate into chondrocytes, which form cartilage anlagen of the future bone. The chondrocytes proliferate, mature, and become hypertrophic, and eventually calcify. This calcified cartilage is then invaded by osteoclasts, osteoblasts, and blood vessels that resorb the cartilage and replace it with bone matrix. These two processes, chondrogenesis and ossification, are regulated by the multitude of genetic and hormonal factors, growth factors, environment, and nutrition. The growth hormone (GH)/insulin-like growth factor-1 (IGF-1) axis particularly is considered to have an important regulator effect on the growth plate chondrogenesis.

Growth impairment is a major complication of patients with systemic juvenile idiopathic arthritis (sJIA). In sJIA, markedly elevated interleukin (IL)-6, which binds to gp130 and to IL-6 receptor to elicit the inflammatory response, appears to be the main causative agent of the inflammation, and we have already reported that the anti-IL-6 receptor monoclonal antibody, tocilizumab, effectively blocks the inflammatory manifestations and the surrogate markers, CRP and serum amyloid A, and that it also induces catch-up growth in sJIA patients [1–3].

Recently the effects of inflammatory cytokines on growth plate chondrocytes have been studied [4–6]. Tumor necrosis factor-α (TNF-α), and IL-1 are considered to directly affect growth plate chondrocytes, but IL-6 is reported to have no direct effect on growth plate chondrocyte dynamics. IL-6 has been considered to affect growth through systemic mechanisms that alter the growth hormone/insulin-like growth factor-1 (GH/IGF-I) axis [7,8].

The purpose of the present study was to examine whether IL-6 in fact has direct effects on growth plate chondrogenesis or, as currently considered, dose not. We investigated the effect of IL-6 on the chondrogenic differentiation of the murine chondrocyte embryonal carcinoma cell line, ATDC5. This cell line has been shown to undergo a sequence of events—namely, cell proliferation, synthesis of the extracellular matrix, cellular hypertrophy, mineralization of matrix, localized vascular invasion and apoptosis—that occur during longitudinal bone growth in vivo and, thereby, provides an excellent model for studying the molecular mechanisms underlying the regulation of growth plate maturation and endochondral bone formation [9]. Our investigation of the effect of IL-6 on the ATDC5 cell line has made possible a considerable extension of our understanding of the effect of IL-6 alone at a cellular level on growth plate chondrocytes. In the presence of insulin, ATDC5 cells differentiate into chondrocytes to form cartilage nodules (chondrogenesis), accompanied with the progressive expression of type II collagen, which is the predominant

* Corresponding author. Tel.: +81 45 787 2671; fax: +81 45 787 0461.
E-mail address: shoko92@bf6.so-net.ne.jp (S. Nakajima).

1043-4666/$ - see front matter © 2009 Elsevier Ltd. All rights reserved.
doi:10.1016/j.cyto.2009.05.002

extracellular matrix in the proliferating stage, and then they differentiate into the cells that express type X collagen in the hypertrophic stage [10].

In this study, we examined the effects of IL-6 on cell proliferation by MTT assay, and on differentiation by examination of the expression levels of chondrogenic marker genes including type II collagen, aggrecan, and type X collagen, using quantitative real-time reverse-transcriptase polymerase chain reaction (qRT-PCR).

2. Methods

2.1. Reagents

A murine chondrogenic cell line, ATDC5, was obtained from Riken cell bank (Tsukuba, Japan). Mouse recombinant IL-6 was purchased from R&D systems (Minneapolis, MN, USA). Anti-mouse IL6 receptor antibody (MR16-1) [11] was a generous gift from Dr. Osugi Chugai Pharmaceutical Co., Ltd. (Shizuoka, Japan). PE-conjugated rat anti-mouse IL-6 receptor monoclonal antibody was from BD Biosciences (San Diego, USA) and biotinylated rat anti-mouse gp130 monoclonal antibody and streptavidin PE were from R&D systems. 1:1 mixture of DMEM and Ham's F-12 medium and 5% fetal bovine serum were from Invitrogen (Tokyo, Japan), human transferring, sodium selenite, bovine insulin, ascorbic acid and tripsin/EDTA were from Sigma–Aldrich (Tokyo, Japan). MTT working solution was from Cosmo Bio Co., Ltd. (Tokyo, Japan) and DSMO was from Sankyo Chemical Co., Ltd. (Nagoya, Japan).

2.2. Analysis of IL-6 receptor and gp130 expressions on ATDC5 cells

FACS analysis was performed to detect IL-6 receptor and gp130 on ATDC5 cells. Following detachment of ATDC5 cells with trypsin/EDTA at Day 0 and Day 2, the cells (1×10^6 cells/ml) were incubated with PE-conjugated rat anti-mouse IL-6 receptor monoclonal antibody and biotinylated rat anti-mouse gp130 monoclonal antibody, which was revealed using streptavidin PE. Mouse spleen cells were assessed as controls. The flow cytometer used in this study was a FACSCAN (BD Biosciences), and the software used for collection and analysis of the results was the program CellQuest ProTM (BD Biosciences).

2.3. Cell culture and stimulation

ATDC5 cells were cultured in a 1:1 mixture of DMEM and Ham's F-12 medium supplemented with 5% fetal bovine serum, 10 μg/ml human transferrin, 3×10^{-8} M sodium selenite, and antibiotics (100 U/ml penicillin G and 100 μg/ml streptomycin sulfate) at 37 °C in a humidified atmosphere of 5% CO_2 in air. In the present study, ATDC5 cells were plated at an initial cell density of 1.0×10^4 cells/cm^2 in 12-multiwell plastic plates (Corning, New York, USA), grown to 70–80% confluency in the culture medium, and then differentiation was induced by the addition of bovine insulin (10 μg/ml) and ascorbic acid (20 μg/ml) to the culture medium (culture Day 0). (To examine the effect of IL-6 on proliferation and differentiation of ATDC5 cells,) the culture medium was replaced every other day from Day 2 to Day 14 with or without the medium containing mouse recombinant IL-6 at various concentrations (1–100 ng/ml). Cultures at least in triplicate were used for each test.

For the experiment of interrupting the complex formation between IL-6 and IL-6 R, ATDC5 cells were preincubated (from Day 2 to Day 14) with anti-mouse IL-6 receptor monoclonal antibody, MR16-1, for 30 min added at concentrations from 0.1 to 10 μg/ml before each time that the culture medium was replaced. Every time, after this was done, fresh medium containing 100 ng/ml mouse recombinant IL-6 was added.

Table 1
Primer sequences for mouse type II collagen, aggrecan, type X collagen and GAPDH. Sequence of the primers used for RT-PCR experiments.

Target	Forward primer (5′–3′)	Reverse primer (5′–3′)
Type II collagen	AAGACCGTCATCGAGTACCGA	ACTGCGGTTGGAAAGTGTTTG
Aggrecan	AACTTCTTTGCCACCGGAGA	GGTGCCCTTTTTACACGTGAA
Type X collagen	GCAGCATTACGACCCAAGAT	TCTGTGAGCTCCATGATTGC
GAPDH	CAAAATGGTGAAGGTCGGTGTG	ATTTGATGTTAGTGGGGTCTCG

2.4. Cell proliferation assays

Cell proliferation was assessed by MTT assay, conducted at Days 0, 2, 6, 10, and 14. ATDC5 cells were plated in 12-well plates and cultured as previously described in the presence of mouse recombinant IL-6 (100 ng/ml). Culture wells were incubated with 1 ml of MTT working solution for 2 h at 37 °C. After removal of MTT working solution, culture wells were incubated with 1 ml of DMSO for 30 min at 37 °C, then 200 μl of supernatants were transferred into each well of a new 96-well microplate and the absorbance at 570 nm was measured with a spectrophotometer (Bio-Rad Model 550). The experiment was performed at least six times, and the results are expressed as means ± standard deviations.

2.5. Cartilaginous nodule formation under a phase-contrast microscope (×100)

Cartilaginous nodule formation was assessed under a phase-contrast microscope (Olympus CKX41) at Day 10.

2.6. Quantitative real time reverse-transcriptase polymerase chain reaction (qRT-PCR) of chondrogenic marker gene expression

The expression levels of chondrogenic marker genes; type II collagen, aggrecan and type X collagen mRNAs were measured at Days 6, 10, and 14 by means of qRT-PCR in ATDC5 cells cultured with 100 ng/ml mouse recombinant IL-6. Total RNA was prepared from the cultures using an RNeasy Mini Kit (Qiagen), and then qRT-PCR was carried out in an ABI Prism 7500 (Applied Biosystems, Foster, CA, USA) with a SuperScript III platinum SYBR Green One-Step qRT-PCR kit (Invitrogen). Primer sequences are listed in Table 1. The cycling profile was 95 °C for 15 s, 55 °C for 30 s, 72 °C for 34 s for 40 cycles. The number of template copies present at the start of the reaction was determined by comparison to a standard scale prepared from mouse genomic DNA. For normalization of the RNA loading, an RT-PCR of GAPDH was also performed in each RT-PCR reaction as an internal control. The abundance of each gene was determined relative to GAPDH. The expression level of each target gene was calculated by standardizing the target gene copy number with the GAPDH copy number in a sample. The analysis of the results is based on triplicate (or more) samples.

2.7. Statistical analysis

Statistical significance was assessed by one-way analysis of variance and Mann–Whitney's *U*-test. Data are reported as the mean ± SD, and are considered significantly different at $P < 0.05$.

3. Results

3.1. Expression of IL-6 receptor and gp130 on the surface of ATDC5 cells

We assessed whether ATDC5 cells express IL-6 receptor and gp130 on their surface by flow cytometry. Although the levels of membrane-anchored IL-6 receptor on ATDC5 cells were much

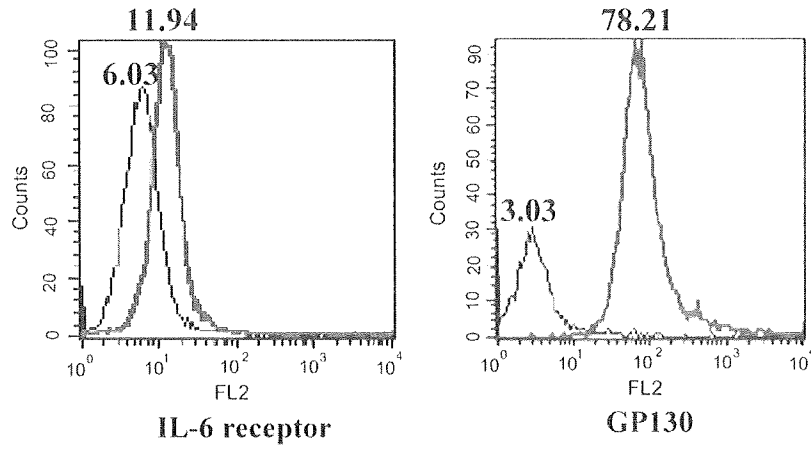

Fig. 1. FACS analysis for expression of IL-6 receptor and gp130 on the surface of ATDC5 cells.

lower than those on mouse spleen cells, we confirmed that ATDC5 cells express both IL-6 receptor and gp130 on their surface. (Fig. 1).

3.2. Molecular changes during the process of differentiation in ATDC5 cells

Chondrogenic differentiation of ATDC5 cells was further characterized by expression of cartilage-characteristic extracellular matrix genes such as aggrecan, type II collagen and type X collagen. In Fig. 2, we outlined the molecular changes of ATDC5 cells during the process of differentiation in the presence of insulin. On Day 2, ATDC5 cells express neither type II collagen nor aggrecan mRNA, but on Day 6, they express both type II collagen and aggrecan mRNA. On Day10, the expression levels of type II collagen and aggrecan gradually decrease while the expression level of type X collagen increases. On Day14, ATDC5 cells express type X collagen substitute for type II collagen.

3.3. Effect of IL-6 on chondrogenic marker gene expression in ATDC5 cells at various concentrations (1–100 ng/ml)

The results of qRT-PCR of the chondrogenic marker gene showed that IL-6 reduced type II collagen and type X collagen gene expression in a dose-dependent manner on Days 6 and 14, respectively (Fig. 3).

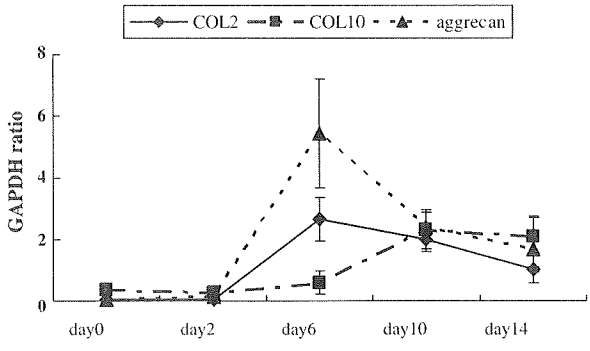

Fig. 2. Molecular changes during the process of differentiation in ATDC5 cells. The molecular changes of ATDC5 cells during the process of differentiation in the presence of insulin were outlined. On Day 2, ATDC5 cells express neither type II collagen nor aggrecan mRNA, but on Day 6, they express both type II collagen and aggrecan mRNA. On Day 10, the expression levels of type II collagen and aggrecan gradually decrease while the expression level of type X collagen increases. On Day 14, ATDC5 cells express type X collagen substitute for type II collagen.

3.4. Effect of IL-6 on cell proliferation in ATDC5 cells

The results of the MTT assay revealed that IL-6 has no inhibitory effect on cell proliferation in ATDC5 cells. The absorbance each day did not differ between the cells cultured with and without IL-6 ($P > 0.05$) (Fig. 4).

3.5. Effect of IL-6 on cartilaginous nodule formation in ATDC5 cells

In control cultures, cartilage nodules were formed at Day 10, but continual exposure of 100 ng/ml of mouse recombinant IL-6 to the culture caused cell flattening and completely inhibited cellular condensation and subsequent formation of cartilage nodules. Pretreatment of undifferentiated ATDC5 cells with 10 μg/ml of MR16-1 neutralized the effect of IL-6, resulting in the formation of cartilage nodules, but pretreatment with 0.001 μg/ml of MR16-1 did not block the effect of IL-6 (Fig. 5).

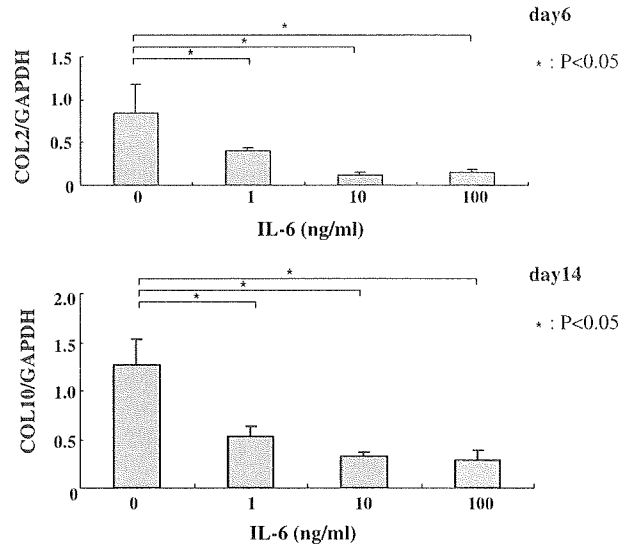

Fig. 3. Effect of IL-6 on the expression of type II collagen and type X collagen at various concentrations (1–100 ng/ml). IL-6 reduced type II collagen and type X collagen gene expression in a dose-dependent manner on Days 6 and 14, respectively. The data represents the mean ± SD from tests of samples in triplicate. $P < 0.05$ vs. control.

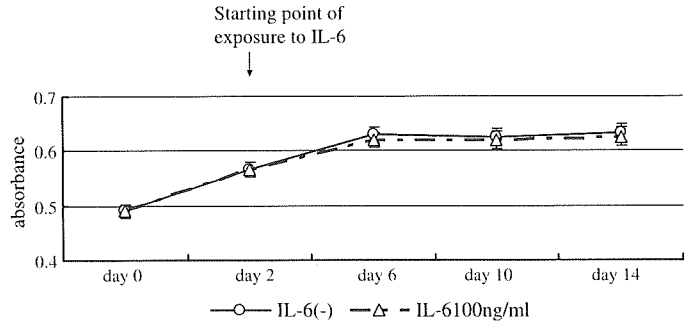

Fig. 4. MTT assay of ATDC5 cells cultured with or without IL-6. The absorbance each day did not differ between the cells cultured with and without IL-6.

3.6. Effect of IL-6 on chondrogenic marker gene expression in ATDC5 cells

The results of qRT-PCR of the chondrogenic marker gene showed that IL-6 (100 ng/ml) markedly reduced type II collagen gene expression on Days 6, 10 and 14, and reduced aggrecan gene expression on Day 6. The results also indicated that MR16-1 blocked the effect of IL-6 to increase both type II collagen and aggrecan gene expression in a dose-dependent manner (Fig. 6A and B). IL-6 (100 ng/ml) also markedly reduced type X collagen gene expression on Days 10 and 14, but MR16-1 inhibited the reduction of type X collagen gene expression dose-dependently (Fig. 6C).

4. Discussion

The present study found that IL-6 inhibited the differentiation of ATDC5 cells. This is the first report describing the inhibitory effect of IL-6 on differentiation of the chondroprogenitor cell line, ATDC5.

Generally, the ATDC5 cell line is an excellent model for studying the molecular mechanisms underlying the regulation of growth plate maturation and endochondral bone formation [9]. At the epiphyseal end of the growth plate, the reserve zone, also called the germinal or stem cell zone, contains the resting chondrocytes [10]. These cells have recently been shown to be crucial for orientation of the underlying columns of chondrocytes and therefore for unidirectional bone growth, probably through the secretion of a growth plate-orienting factor [12]. Upon some unknown trigger, the stem cells enter the proliferating zone, and local and systemic factors regulate longitudinal bone growth, which involves the differentiation of committed stem cells into proliferating chondrocytes (early chondrogenesis); after a finite number of cell divisions, these cells finally differentiate into the hypertrophic phenotype that deposits a matrix that is mineralized and eventually replaced by bone [13,14]. The ATDC5 cell line allows the study of two critical events during cartilage formation: the early differentiation of committed stem cells into chondrocytes and the terminal differentiation of proliferating to hypertrophic chondrocytes [15]. We showed the molecular changes during the process of differentiation of ATDC5 cells in the presence of insulin in Fig. 2. In this study, we investigate the effect of IL-6 especially on early chondrogenesis; the differentiation of commit-

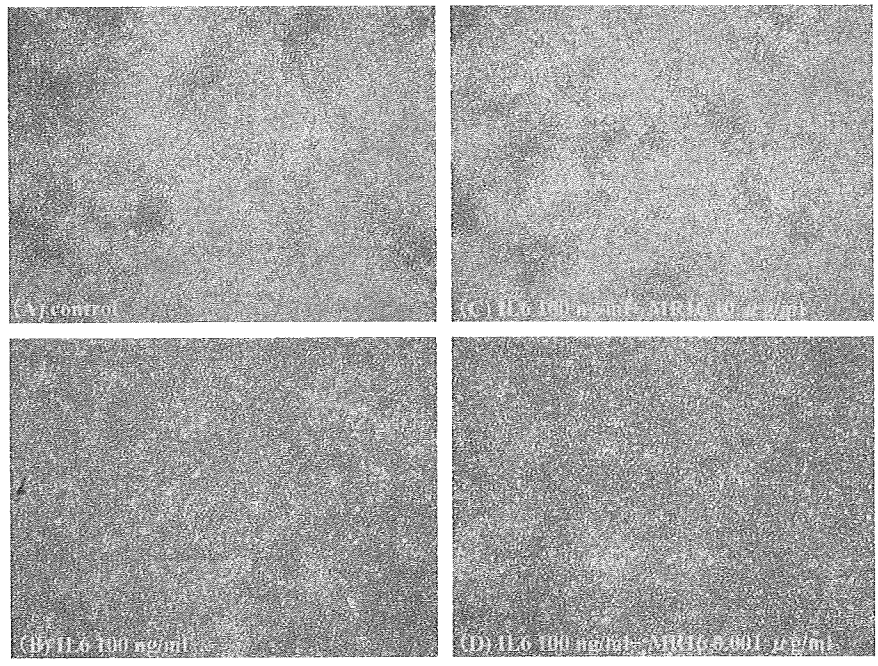

Fig. 5. Phase-contrast micrographs of ATDC5 cells with and without IL-6 at Day 10. In the absence of IL-6 (control), typical cartilage nodules are formed (A). The cells having continual exposure to 100 ng/ml of mouse recombinant IL-6 are flattened, and their cellular condensation and subsequent formation of cartilaginous nodules are completely inhibited (B). After pretreatment with 10 μg/ml of MR16-1, cartilage nodules are formed (C), but those cells pretreated with 0.001 μg/ml of MR16-1 are flattened (D).

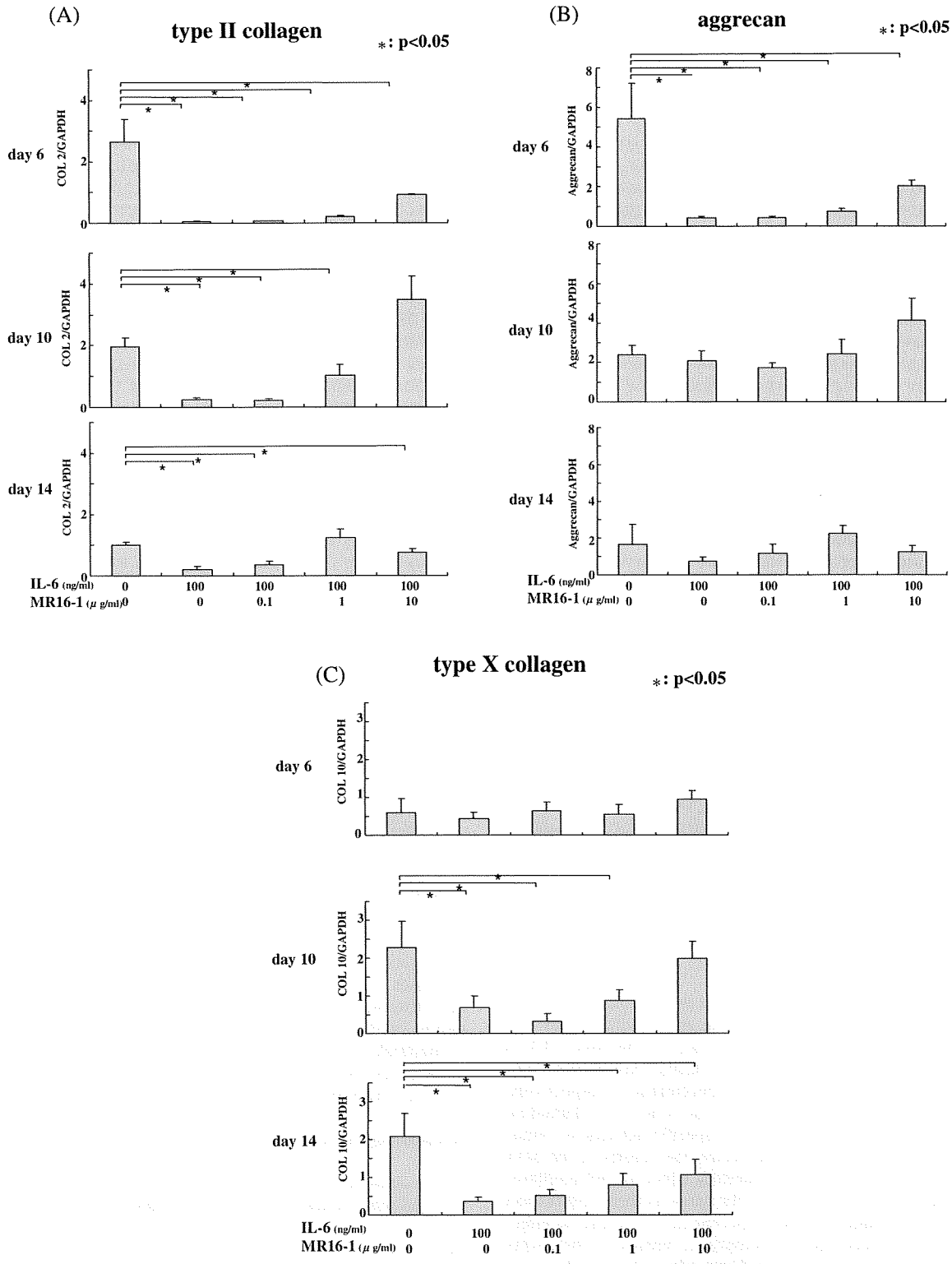

Fig. 6. Effect of IL-6 on chondrogenic marker gene expression in ATDC5 cells. IL-6 (100 ng/ml) markedly reduced type II collagen gene expression on Days 6, 10 and 14, and MR16-1 blocked the effect of IL-6 to increase type II collagen gene expression in a dose-dependent manner (A). IL-6 markedly reduced aggrecan gene expression on Day 6 and MR16-1 blocked the effect of IL-6 to increase aggrecan gene expression in a dose-dependent manner (B). IL-6 also markedly reduced type X collagen gene expression on Days 10 and 14 but MR16-1 inhibited the reduction of type X collagen gene expression dose-dependently (C). The data represents the mean ± SD from tests of samples in triplicate or more. COL 2: type II collagen, COL 10: type X collagen.

ted stem cells into proliferating chondrocytes in the ATDC5 cell line.

The first evidence that IL-6 inhibits the differentiation of ATDC5 cells is that IL-6 was found to inhibit cartilaginous nodule forma-

tion. The processes of cellular condensation and subsequent cartilaginous nodule formation are important prerequisites for initiation of chondrogenesis in mesenchymal cell cultures. In the presence of insulin, ATDC5 cells lose contact inhibition of movement and grow beyond confluence to produce two or three layers of cells in a process known as cartilaginous nodule formation. The results shown in Fig. 5 indicate that IL-6 inhibits cartilaginous nodule formation. The second piece of evidence for the inhibitory effect of IL-6 on the differentiation of ATDC5 cells is that IL-6 markedly reduced the expression of type II collagen, aggrecan and type X collagen, when IL-6 was continuously added to the culture system of ATDC5 from Day 2.

Some previous studies have assessed whether pro-inflammatory cytokines including IL-1, TNF-α, and IL-6 could act at a cellular level on the growth plate chondrocytes [4–6]. IL-6 has been considered not to have any direct effect on growth plate chondrocyte dynamics, but to inhibit growth plate chondrogenesis and longitudinal growth by reducing the systemic effects of IGF-1 [7,8]. But we have shown that IL-6 has directly inhibited the differentiation of the chondroprogenitor cell line, ATDC5 in its early stage. Our observations in the present study raise the possibility that IL-6 may affect committed stem cells at a cellular level during chondrogenic differentiation of growth plate chondrocytes.

There is a possible reason that the results of the present experiment differed from those of earlier experiments, namely, that the timing of the addition of IL-6 to the culture system was different. In the present study, to assess the effect of IL-6 on committed stem cells, IL-6 was added to the culture medium from Day 2, a time when ATDC5 cells have not yet expressed much type II collagen mRNA—in short, they have not differentiated into proliferative chondrocytes. In the previous study, IL-6 was added to the culture medium, in which ATDC5 cells have already differentiated and have entered the proliferative stage, expressing a large amount of type II collagen mRNA [6]. We also recognized that when we added IL-6 to the culture medium from Day 6, ATDC5 cells differentiated into hypertrophic cells and expressed type X collagen mRNA on Day 14 in the same way as the control. On Day 6, ATDC5 cells had already differentiated into proliferative chondrocytes, expressing type II collagen mRNA. After all, IL-6 has no effect on ATDC5 cells, when they have already differentiated and reached the proliferative stage. In this respect, we recognized the same process as in the previous study. The main finding of our study is that only undifferentiated cells, that is, committed stem cells, are inhibited from differentiation into proliferative and subsequent hypertrophic chondrocytes by IL-6.

Horan et al. investigated the effects of pro-inflammatory cytokines on both rat costochondral resting zone chondrocytes and growth zone chondrocytes [4]. They evaluated the effect of IL-6 on (H3)-thymidine incorporation and alkaline phosphatase-specific activity for proliferation and differentiation, respectively, and they reported that IL-6 had no effect on either (H3)-thymidine incorporation or alkaline phosphatase-specific activity in either type of chondrocytes. First, in our study, the results of the MTT assay revealed that IL-6 has no inhibitory effect on cell proliferation in ATDC5 cells. Our result was the same as their observation in this respect. In addition, they reported that IL-6 had no effect on alkaline phosphatase-specific activity, in contrast to the effects observed with IL-1, which promoted the differentiation of resting zone cells. These results will be supported by our observation that IL-6 inhibits the differentiation of committed stem cells into the proliferative stage in ATDC5 cell line.

It was reported that a reduction in metatarsal growth was not noticed after 8 days' exposure to IL-6, although a reduction in metatarsal growth was seen after exposure to TNF-α and IL-1β [6]. IL-6 did not affect longitudinal growth in an organ culture system of neonatal mouse metatarsal bones in that study. However, we suspect that a reduction in metatarsal growth with exposure to IL-6 could have occurred given a longer time period of observation. IL-6 affects only committed stem cells, which do not contribute directly to longitudinal growth because the chondrocytes do not proliferate [16,17]. Moreover, the cells already differentiated into proliferating and hypertrophic zones can continue their differentiation. For the reasons stated above, a reduction in metatarsal growth might not be noted immediately after 8 days exposure to IL-6. On the other hand, TNF-α and IL-1β are already known to affect proliferative zone cells, which contribute directly to longitudinal growth.

Growth impairment is a major complication for chronic inflammatory diseases, and many reasons for growth impairment in chronic illness have been considered, such as malnutrition, hormone deficiency, glucocorticoids and inflammatory cytokines [18,19]. Systemic JIA is one of the chronic inflammatory diseases characterized by severe multi-organ diseases and growth impairment. In sJIA, IL-6 is one of the major causative agents for systemic inflammation and growth impairment. Recent trials of the anti-IL-6 receptor monoclonal antibody, tocilizumab, for patients with sJIA indicated that tocilizumab blocks IL-6/IL-6 receptor-mediated inflammation, and that the growth impairment is overcome, resulting in catch-up growth [1,2,20]. Moreover, in a recent study, the transgenic mice over-expressing IL-6 experienced a stunted growth rate, and neutralization of IL-6 activity by a MAb produced a partial improvement of the animals' growth rate [7]. De Benedetti et al. reported that IL-6 inhibits growth plate chondrogenesis and longitudinal growth by reducing the systemic effects of IGF-1 [21]. But the ATDC5 cell line that we used in the present study, is a simple culture model for investigating the cellular-level effect of IL-6 on the differentiation of growth plate chondrocytes without considering any other factors including glucocorticoids or systemic IGF-1. Also, the results of our study using this simple culture model indicated that IL-6 directly inhibited early differentiation of ATDC5 cells at a cellular level.

5. Conclusion

This study demonstrates that IL-6 inhibits the early differentiation of ATDC5 cells, suggesting, in clinical terms, that IL-6 directly inhibits early differentiation of growth plate chondrocytes, and that growth impairment in sJIA may be brought about in partially through the direct inhibitory effect of IL-6 on committed stem cells in the growth plate. In sJIA patients, committed stem cells in the growth plate may be inhibited by IL-6 from differentiation into proliferative chondrocytes, and consequently, the normal processes of bone development followed by differentiation into hypertrophic chondrocytes and the mineralization of matrix may also be inhibited. We believe that the therapeutic strategies using tocilizumab to target the IL-6/IL-6 receptor process, which effectively block the inflammatory manifestations in sJIA, are likely to achieve return to normal growth.

Acknowledgments

The authors thank Mr. C. W. P. Reynolds for linguistic assistance with this manuscript and Mr. Yoshiyuki Ohsugi for his generous gift.

References

[1] Yokota S, Miyamae T, Imagawa T, Iwata N, Katakura S, Mori M. Inflammatory cytokines and systemic-onset juvenile idiopathic arthritis. Mod Rheumatol 2004;14:12–7.
[2] Yokota S, Miyamae T, Imagawa T, Katakura S, Kurosawa R, Mori M. Clinical study of tocilizumab in children with systemic-onset juvenile idiopathic arthritis. Clin Rev Allergy Immunol 2005;28:231–8.
[3] Yokota S, Imagawa T, Mori M, Miyamae T, Aihara Y, Takei S, et al. Efficacy and safety of tocilizumab in patients with systemic-onset juvenile idiopathic arthritis: a randomised, double-blind, placebo-controlled, withdrawal phase III trial. Lancet 2008;371:998–1006.

[4] Horan J, Dean DD, Kieswetter K, Schwartz Z, Boyan BD. Evidence that interleukin-1, but not interleukin-6, affects costochondral chondrocyte proliferation, differentiation, and matrix synthesis through an autocrine pathway. J Bone Miner Res 1996;11:1119–29.
[5] Martensson K, Chrysis D, Savendahl L. Interleukin-1beta and TNF-alpha act in synergy to inhibit longitudinal growth in fetal rat metatarsal bones. J Bone Miner Res 2004;19:1805–12.
[6] MacRae VE, Farquharson C, Ahmed SF. The restricted potential for recovery of growth plate chondrogenesis and longitudinal bone growth following exposure to pro-inflammatory cytokines. J Endocrinol 2006;189:319–28.
[7] De Benedetti F, Meazza C, Oliveri M, Pignatti P, Vivarelli M, Alonzi T, et al. Effect of IL-6 on IGF binding protein-3: a study in IL-6 transgenic mice and in patients with systemic juvenile idiopathic arthritis. Endocrinology 2001;142:4818–26.
[8] Lieskovska J, Guo D, Derman E. IL-6-overexpression brings about growth impairment potentially through a GH receptor defect. Growth Horm IGF Res 2002;12:388–98.
[9] Shukunami C, Ishizeki K, Atsumi T, Ohta Y, Suzuki F, Hiraki Y. Cellular hypertrophy and calcification of embryonal carcinoma-derived chondrogenic cell line ATDC5 in vitro. J Bone Miner Res 1997;12:1174–88.
[10] van der Eerden BC, Karperien M, Wit JM. Systemic and local regulation of the growth plate. Endocr Rev 2003;24:782–801.
[11] Okazaki M, Yamada Y, Nishimoto N, Yoshizaki K, Mihara M. Characterization of anti-mouse interleukin-6 receptor antibody. Immunol Lett 2002;84:231–40.
[12] Abad V, Meyers JL, Weise M, Gafni RI, Barnes KM, Nilsson O, et al. The role of the resting zone in growth plate chondrogenesis. Endocrinology 2002;143:1851–7.
[13] Green H, Morikawa M, Nixon T. A dual effector theory of growth-hormone action. Differentiation 1985;29:195–8.
[14] Isaksson OG, Ohlsson C, Nilsson A, Isgaard J, Lindahl A. Regulation of cartilage growth by growth hormone and insulin-like growth factor I. Pediatr Nephrol 1991;5:451–3.
[15] Cancedda R, Descalzi Cancedda F, Castagnola P. Chondrocyte differentiation. Int Rev Cytol 1995;159:265–358.
[16] Brighton CT. Structure and function of the growth plate. Clin Orthop Relat Res 1978:22–32.
[17] Iannotti JP. Growth plate physiology and pathology. Orthop Clin North Am 1990;21:1–17.
[18] MacRae VE, Wong SC, Farquharson C, Ahmed SF. Cytokine actions in growth disorders associated with pediatric chronic inflammatory diseases (review). Int J Mol Med 2006;18:1011–8.
[19] De Luca F. Impaired growth plate chondrogenesis in children with chronic illnesses. Pediatr Res 2006;59:625–9.
[20] Yokota S, Miyamae T, Imagawa T, Iwata N, Katakura S, Mori M, et al. Therapeutic efficacy of humanized recombinant anti-interleukin-6 receptor antibody in children with systemic-onset juvenile idiopathic arthritis. Arthritis Rheum 2005;52:818–25.
[21] De Benedetti F, Alonzi T, Moretta A, Lazzaro D, Costa P, Poli V, et al. Interleukin 6 causes growth impairment in transgenic mice through a decrease in insulin-like growth factor-I. A model for stunted growth in children with chronic inflammation. J Clin Invest 1997;99:643–50.

Double-Stranded RNA and TGF-α Promote MUC5AC Induction in Respiratory Cells

Hiromi Tadaki,*† Hirokazu Arakawa,[1]* Takahisa Mizuno,* Tomoko Suzuki,* Kiyoshi Takeyama,‡ Hiroyuki Mochizuki,* Kenichi Tokuyama,§ Shumpei Yokota,† and Akihiro Morikawa*

Viral infection is a major trigger for exacerbation of asthma and induces overproduction of mucins. We investigated whether dsRNA could amplify the induction of mucin by TGF-α in human bronchial epithelial cells, as well as the molecular mechanisms regulating MUC5AC expression. Human pulmonary mucoepidermoid carcinoma (NCI-H292) cells and normal human bronchial epithelial cells were exposed to polyinosinic-cytidyric acid (poly(I:C)) and TGF-α. Then, MUC5AC protein production, mRNA expression, and promoter activity were evaluated. Cells were pretreated with a selective inhibitor of ERK, and phosphorylation of ERK was examined by Western blotting. Furthermore, the expression of MAPK phosphatase 3 (MKP3) mRNA was evaluated and the effect of MKP3 overexpression was assessed. Poly(I:C) synergistically increased MUC5AC induction by TGF-α in both NCI-H292 and normal human bronchial epithelial cells. This increase was dependent on MUC5AC gene transcription. A MEK1/2 inhibitor (U0126) significantly inhibited MUC5AC production. Phosphorylation of ERK was enhanced by poly(I:C). TGF-α stimulation up-regulated MKP3 mRNA expression, while costimulation with poly(I:C) inhibited this up-regulation dose-dependently. Enhanced expression of MUC5AC mRNA by poly(I:C) in wild-type cells was completely suppressed in cells transfected with the MKP3 expression vector. dsRNA can synergistically amplify the induction of MUC5AC mucin by TGF-α. This synergistic effect on MUC5AC production may be due to enhanced activation of ERK through inhibition of MKP3 by poly(I:C). ***The Journal of Immunology,*** **2009, 182: 293–300.**

In chronic airway diseases such as asthma, goblet-cell hyperplasia is an important feature (1). Excessive secretion of mucus by hyperplastic goblet cells causes airway plugging and contributes to morbidity and mortality in asthma patients (2, 3). To date, 19 different mucin genes have been identified. Among these, MUC5AC mucin is a major component of the mucus produced by airway epithelial cells (4), and its production is regulated by epidermal growth factor receptor (EGFR) signaling pathway (5, 6). EGFR and its ligands are not only expressed in patients with malignant lung tumors, but also in those with airway inflammatory diseases such as asthma (7). TGF-α is one of the ligands of EGFR, and it is known to play a critical role in phosphorylation of EGFR that leads to MUC5AC production in the airways (5).

Viral infection is a common cause of the exacerbation of asthma. Among the many viruses that infect the airways, human rhinovirus, respiratory syncytial virus, influenza virus, and parainfluenza virus are particularly common pathogens that induce the hypersecretion of mucus and exacerbation of asthma (8–10). These are RNA viruses that synthesize dsRNA during replication in infected cells. TLR3 recognizes dsRNA and was the first antiviral TLR identified (11). Because dsRNA is a universal viral molecule, TLR3 has been assumed to have a central role in the host response to infection by viruses (11). Previous studies have shown that stimulation with a synthetic analog of viral dsRNA (poly inosinic-cytidyric acid, poly(I:C))[2] is mediated by a pathway involving TLR3 that induces airway inflammation due to various cytokines and chemokines such as IL-8, IL-6, and RANTES (12). Despite the importance of excessive mucin production due to viral infection in triggering the exacerbation of asthma, the mechanisms causing such overproduction remain unknown.

We hypothesized that viral infection might synergistically amplify respiratory mucin gene expression and protein production induced by growth factors that are involved in the pathogenesis of asthma. Here, we demonstrate that a synthetic analog of viral dsRNA (poly(I:C)) synergistically increases the induction of respiratory mucin MUC5AC by TGF-α in human airway epithelial cells, both at the level of mRNA expression and protein production. This action depends on the activation of ERK, and the ERK pathway is enhanced through inhibition of MAPK phosphatase 3 (MKP3) by poly(I:C).

Materials and Methods

Cell culture and stimulation

A human pulmonary mucoepidermoid carcinoma cell line (NCI-H292) was maintained in RPMI 1640 medium supplemented with 10% FBS, penicillin (100 U/ml), and streptomycin (100 μg/ml) at 37°C in a humidified atmosphere with 5% CO_2. NCI-H292 cells were seeded into 12-well plates for the ELISA and luciferase assay, and into 6-cm dishes for Western blotting and mRNA analysis. Cells were grown until 70% confluence was reached,

*Department of Pediatrics and Developmental Medicine, Gunma University Graduate School of Medicine, Gunma, Japan; †Department of Pediatrics, Yokohama City University School of Medicine, Kanagawa, Japan; ‡First Department of Medicine, Tokyo Women's Medical University, Tokyo, Japan; and §Department of Pharmacy, Takasaki University of Health and Welfare, Gunma, Japan

Received for publication July 10, 2008. Accepted for publication October 23, 2008.

The costs of publication of this article were defrayed in part by the payment of page charges. This article must therefore be hereby marked *advertisement* in accordance with 18 U.S.C. Section 1734 solely to indicate this fact.

[1] Address correspondence and reprint requests to Dr. Hirokazu Arakawa, Department of Pediatrics and Developmental Medicine, Gunma University Graduate School of Medicine, 3-39-15 Showa-machi, Maebashi, Gunma 371-8511, Japan. E-mail address: harakawa@showa.gunma-u.ac.jp

[2] Abbreviations used in this paper: poly(I:C), polyinosinic-cytidyric acid; AB-PAS, Alcian blue/periodic acid-Schiff; C_T, threshold cycle; EGFR, epidermal growth factor receptor; MKP, MAPK phosphatase; NHBE, normal human bronchial epithelial; RT, room temperature.

Table I. *Primers used for quantitative real-time PCR analysis of gene expression*

Target mRNA	Forward Primer (5′ to 3′)	Reverse Primer (3′ to 5′)
MUC5AC	TCA CAG CCG GGT ACG CGT TGG CAC AAG TGG	TGC TAT TAT GCC CTG TGT AGC CAG GAC TGC
β-actin	GTG GGG CGC CCC AGG CAC CA	CTC CTT AAT GTC ACG CAC GAT TTC
MKP3	CAC CGA CAC AGT GGT GCT CT	CTG AAG CCA CCT TCC AGG TAG
EGFR	TGC GTC TCT TGC CGG AAT	GGC TCA CCC TCC AGA AGG TT

and they were maintained overnight in serum-free medium before stimulation. Cells were exposed to poly(I:C) (Sigma-Aldrich) at 25 μg/ml or TGF-α (R&D Systems) at 4 ng/ml, or to a combination of both agents.

Normal human bronchial epithelial (NHBE) cells were purchased from Lonza. NHBE cells were seeded at density of $1.3 \times 10^5/cm^2$ into 12-well plates containing bronchial epithelial growth medium (Lonza) supplemented with defined growth factors and retinoic acid from the SingleQuot kit (Lonza), and were incubated at 37°C in a humidified atmosphere with 5% CO_2. Cells were exposed to poly(I:C) (25 μg/ml) or TGF-α (4 ng/ml), or a combination of both agents, for 24 h.

Analysis of mucin

NCI-H292 cells were stained with Alcian blue and periodic acid-Schiff stains (AB-PAS). MUC5AC protein was measured as described previously (5). In brief, supernatants were collected at 24 h after stimulation and cell lysates were prepared with PBS, and 50 μl of each sample was incubated with bicarbonate-carbonate buffer (50 μl) at 40°C in a 96-well plate (Nunc) overnight. Plates were washed three times with PBS and blocked with 2% BSA for 1 h at 37°C. Plates were again washed three times with PBS and then incubated with 50 μl of mouse monoclonal anti-MUC5AC Ab (1/100) (Lab Vision/NeoMarkers), which was diluted with PBS containing 0.05% Tween 20 and dispensed into each well. After 1 h, the plates were washed three times with PBS, and 100 μl of HRP-sheep anti-mouse IgG conjugate (1/10,000) (Amersham Biosciences) was added to each well. After 1 h, the plates were washed three times with PBS. Color was developed with 3,3′,5,5′-tetramethylbenzidine peroxidase solution (Kirkegaard & Perry Laboratories) and the reaction was stopped with 1 M H_2SO_4. The data were expressed as a fold induction on the same experimental day due to various mucin production with cell passage in NCI-H292 cells.

Real-time quantitative PCR analysis

Expression of MUC5AC, MKP3, and EGFR mRNA by NCI-H292 cells was determined by reverse transcription (RT), followed by the real-time quantitative PCR. Total RNA was extracted from lysates of differentiated NCI-H292 cells using Isogen (Nippon Gene) at 12 h after stimulation. RT was performed with 1 μg of total RNA and oligo(dT) primers in a 25-μl reaction mixture according to the manufacturer's protocol (Applied Biosystems). The sequences of the specific primer sets that were used for PCR are listed in Table I (13, 14).

Real-time PCR was performed with an ABI Prism 7900HT sequence detection system (Applied Biosystems) using SYBR Green (Applied Biosystems) as a dsDNA-specific binding dye. For MUC5AC and β-actin, initial denaturation was done at 95°C for 10 min, followed by 40 cycles of denaturation at 95°C for 15 s and annealing and extension at 60°C for 1 min. The threshold cycle (C_T) was recorded for each sample to reflect the level of mRNA expression. A validation experiment confirmed linear dependence of the C_T value on the concentrations of MUC5AC and β-actin and the consistency of ΔC_T (mean C_T for MUC5AC − mean C_T for β-actin) in a given sample at different RNA concentrations. ΔC_T was therefore used as an indicator of relative mRNA expression. To determine the effects of different stimuli on MUC5AC gene expression compared with unstimulated cells, $\Delta\Delta C_T$ was calculated ($\Delta\Delta C_T$ = ΔC_T for stimulated cells − ΔC_T for unstimulated cells). MUC5AC mRNA expression was indexed to β-actin mRNA expression by using the formula $1/(2^{\Delta C_T}) \times 100\%$. $2^{\Delta\Delta C_T}$ was calculated to demonstrate the fold change of MUC5AC gene expression in stimulated cells compared with unstimulated cells.

Expression of MKP3 and EGFR mRNA by NCI-H292 cells was determined in the same manner.

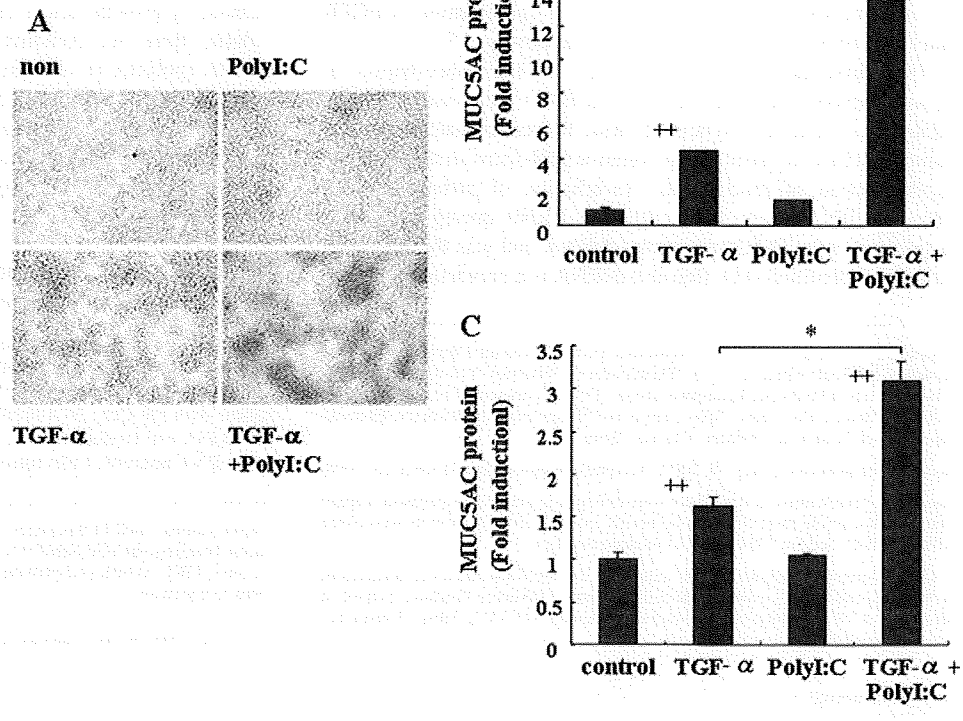

FIGURE 1. Synergistic effect of poly(I:C) and TGF-α on MUC5AC production. *A*, AB-PAS staining of NCI-H292 cells for identification of mucus glycoconjugates. Incubation with poly(I:C) (25 μg/ml) and TGF-α (4 ng/ml) for 24 h increased positive staining. Effect of poly(I:C) (25 μg/ml) on TGF-α (4 ng/ml)-induced MUC5AC mucin production in NCI-H292 cell supernatant ($n = 9$) (*B*) and cell lysate ($n = 9$) (*C*). Cells were incubated with poly(I:C) and TGF-α for 24 h. Data are shown as means ± SD. ++, $p < 0.01$ compared with non-stimulated control cells. *, $p < 0.05$ and **, $p < 0.01$.

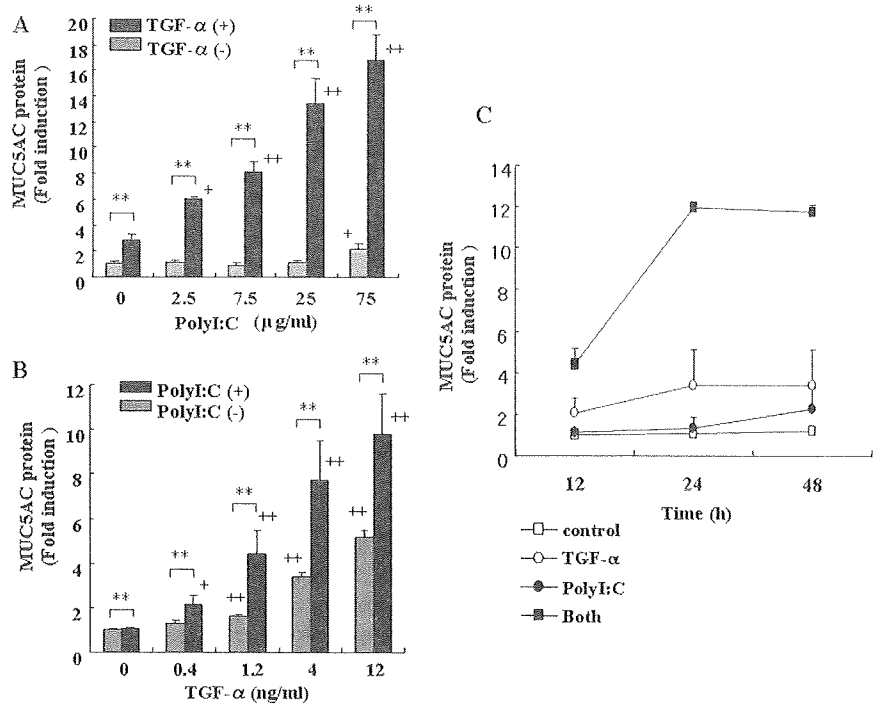

FIGURE 2. Dose responsiveness and time course of MUC5AC protein production. *A*, Effect of the poly(I:C) concentration on TGF-α (4 ng/ml)-induced MUC5AC mucin production in NCI-H292 cells (n = 6). Cells were incubated with poly(I:C) and TGF-α for 24 h. *B*, Effect of the TGF-α concentration on poly(I:C) (25 μg/ml)-induced MUC5AC mucin production in NCI-H292 cells (n = 6). Cells were incubated with poly(I:C) and TGF-α for 24 h. *C*, Effect of poly(I:C) (25 μg/ml) on the time course of induction of MUC5AC mucin production by TGF-α (4 ng/ml) in NCI-H292 cells (n = 6). Data are shown as means ± SD. +, $p < 0.05$ and ++, $p < 0.01$ compared with nonstimulated control cells. **, $p < 0.01$.

Reporter assay for the MUC5AC promoter

To investigate the regions of the MUC5AC promoter that were activated by poly(I:C) and TGF-α, the full-length human MUC5AC promoter was cloned into pGL3basic (a promoterless luciferase vector). This was then serially truncated using a combination of restriction enzyme digestion and PCR amplification to successively isolate regions of the promoter containing a large variety of potential transcription factor-binding sites (−1330 to −63).

NCI-H292 (0.8×10^5) cells were seeded into 12-well plates and grown overnight in complete medium. At 60% confluence, cells were rinsed with 1 ml of serum-free medium and incubated for 1 h. Then the cells were transfected using 1.3 μl of FuGENE 6 (Roche Applied Science) in 50 μl of RPMI 1640 medium per well plus 4 μl of MUC5AC promoter-luciferase plasmid DNA. At 1 h after transfection, cells were stimulated with poly(I:C) (25 μg/ml) and then incubated for 12 h before stimulation with TGF-α (4 ng/ml). Cell lysates were prepared, and reporter gene activity was determined by using a luciferase assay kit (Promega). The total protein concentration of samples was measured by spectrophotometry (NanoDrop from Thermo Scientific) to adjust for variations in harvesting of cells.

Western blot analysis

Cells (3.0×10^5) were washed with PBS and lysed in 300 μl of lysis buffer (0.5% Nonidet P-40, 10 mM Tris-Cl (pH 7.4), 150 mM NaCl, 3 mM *p*-amidinophenylmethanesulfonyl fluoride (Sigma-Aldrich), 5 mg/ml aprotinin (Sigma-Aldrich), 2 mM sodium orthovanadate (Sigma-Aldrich), 5 mM EDTA). Whole-cell extracts were subjected to electrophoresis on 7.5–12% Tris-glycine gel (XV Pantera gel; DRC) and then transferred to Sequi-Blot polyvinylidene difluoride membranes (Immobilon-P; Millipore). Membranes were blocked with 5% skim milk in Tris-buffered saline with 0.05% Tween 20 (TBS-T (pH 7.5)) for 30 min at room temperature (RT) and

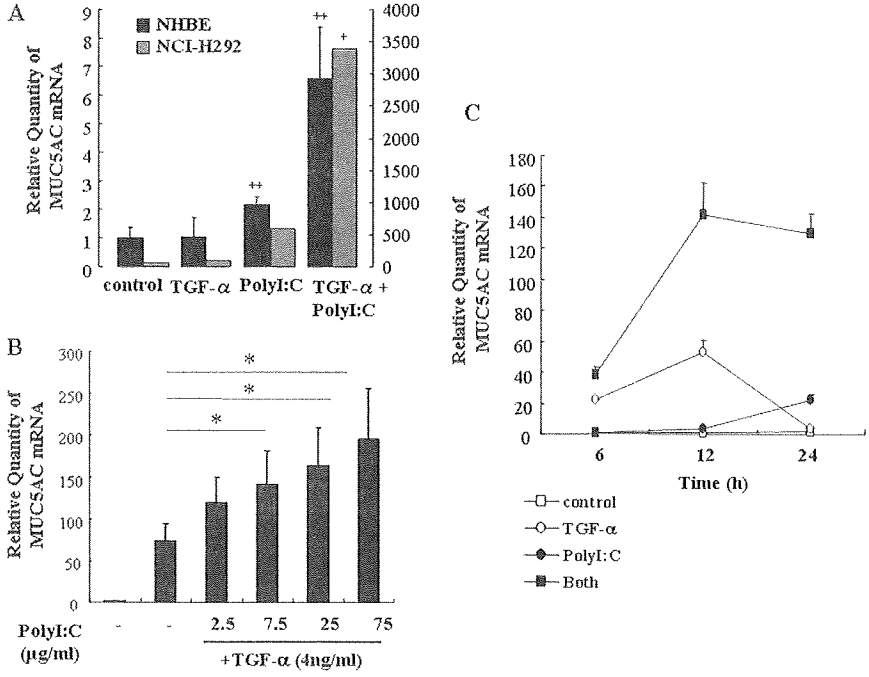

FIGURE 3. Dose responsiveness and time course of MUC5AC mRNA expression. *A*, Effect of poly(I:C) (25 μg/ml) on TGF-α (4 ng/ml)-induced MUC5AC gene expression in NCI-H292 cells and NHBE cells. Cells were incubated with poly(I:C) and TGF-α for 24 h. Data are presented as the fold induction over the level in control NHBE cells. The right side of the *y*-axis is for NCI-H292 cells and the left side is for NHBE cells (n = 6). *B*, Effect of the poly(I:C) concentration on TGF-α (4 ng/ml)-induced MUC5AC mRNA expression in NCI-H292 cells (n = 6). Cells were incubated with poly(I:C) and TGF-α for 12 h. *C*, Effect of poly(I:C) (25 μg/ml) on the time course of induction of MUC5AC mRNA expression by TGF-α (4 ng/ml) in NCI-H292 cells (n = 4). Data are shown as means ± SD. +, $p < 0.05$ and ++, $p < 0.01$ compared with nonstimulated control cells. *, $p < 0.05$.

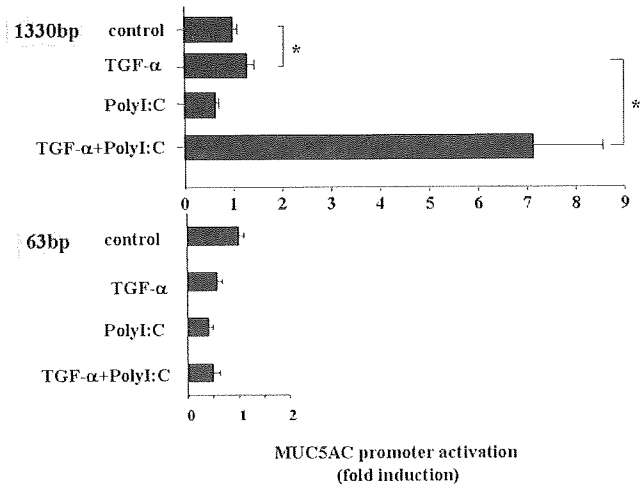

FIGURE 4. Effect of poly(I:C) (25 μg/ml) on TGF-α (4 ng/ml)-induced *trans*-activation of the full-length (−1330) and the short-length (−63) MUC5AC promoter in NCI-H292 cells (n = 6). Data are shown as means ± SD. *, $p < 0.05$.

probed with primary anti-human phospho-p44/42 MAPK (Thr^{202}/Tyr^{204}) Ab and p44/42 MAPK Ab (Cell Signaling Technology) for 1 h at RT. The membranes were then washed with TBS-T and incubated with secondary donkey anti-rabbit Ig Ab conjugated to HRP (Amersham Biosciences) for 1 h at RT. Finally, Ab-Ag complexes were detected using an ECL chemiluminescent detection system according to the manufacturer's instructions (ECL plus Western blot detection system; Amersham Biosciences).

Cloning of MKP3 expression vector and transfection into NCI-H292 cells

A DNA fragment of the coding sequence of MKP3 was amplified by PCR using cDNA from poly(I:C)-treated NCI-H292 cells. The purified PCR product was digested with *Bam*HI and *Sal*I and cloned into the pAcGFP1-C1 vector (Clontech Laboratories). The plasmid was analyzed by digestion with restriction enzymes and DNA sequencing. Plasmids for transfection were purified with HiSpeed Plasmid Maxi kit (Qiagen). H292 cells were seeded into 6-well plates and grown to 50% confluence. Cells were transfected with 4 μg of expression vector with 10 μl of Lipofectamine 2000 (Promega) and grown in RPMI 1640 medium supplemented with 10% FBS, penicillin (100 U/ml), and streptomycin (100 μg/ml). After 24 h, the medium was changed to RPMI 1640 supplemented with 10% FBS without antibiotics. Then, the cells were exposed to poly(I:C) (25 μg/ml), TGF-α (4 ng/ml), or a combination of both agents. After 12 h, the expression of MUC5AC and MKP3 mRNA was evaluated.

Other reagents

U0126 (a MEK1/2 inhibitor) was purchased from Sigma-Aldrich and monoclonal anti-human CXCL8/IL-8 Ab was purchased from R&D Systems. U0126 was dissolved in DMSO, while the monoclonal anti-human CXCL8/IL-8 Ab was dissolved in PBS. In all studies, the concentration of DMSO was 0.02–0.06%. U0126 (20 μM) (15, 16) and the anti-IL-8 Ab (2 μg/ml) were preincubated with cells for 1 h before adding poly(I:C) and TGF-α.

Phosphoprotein assay

Cells (3.0×10^5/ml) were seeded into 6-cm dishes and were treated with poly(I:C) for 1 h and then with TGF-α for 15 min. Protein lysates were prepared by using a cell lysis kit (Bio-Rad), and phosphorylated EGFR was detected with an EGFR (Tyr) assay kit (Bio-Rad) and a phosphoprotein testing reagent kit (Bio-Rad) according to the manufacturer's protocol. Briefly, 50 μl of cell lysate (adjusted to a protein concentration of 200–400 μg/ml) was plated into a 96-well filter plate coated with EGFR Ab-coupled beads and incubated overnight on a platform shaker at 300 rpm at RT. Total protein was measured with a Bio-Rad DC protein assay kit.

Statistical analysis

All data are expressed as the means ± SD. Results were analyzed by using the paired Student's t test or ANOVA as appropriate. Analyses were done with SPSS II software (SPSS Japan), and p values of <0.05 were considered significant.

Results

Poly(I:C) synergistically enhances MUC5AC protein production induced by TGF-α

First, we examined the ability of TGF-α and poly(I:C) to induce mucous glycoconjugate production assessed by AB-PAS staining in NCI-H292 cells (Fig. 1*A*). Twenty-four hours of incubation with TGF-α (4 ng/ml) increased PAS-positive staining, while poly(I:C) (25 μg/ml) alone did not affect staining. However, poly(I:C) enhanced the stimulatory effect of TGF-α on mucous glycoconjugate production (Fig. 1*A*). To quantify the MUC5AC mucin production, an ELISA was performed. TGF-α alone caused a 5-fold increase in MUC5AC mucin protein in cell supernatant (Fig. 1*B*) and a 1.5-fold increase in cell lysate (Fig. 1*C*) from NCI-H292 cells 24 h after stimulation. Poly(I:C) alone caused little increase in MUC5AC mucin protein; however, poly(I:C) strongly potentiated the effect of TGF-α. Thereafter, we evaluated MUC5AC mucin protein only in cell supernatant, because it was more prominent than cell lysate.

Next, we determined effects of dose responses of poly(I:C) (2.5–75 μg/ml) and TGF-α (0.4–12 ng/ml) on MUC5AC mucin production (Fig. 2, *A* and *B*). Although poly(I:C) alone did not

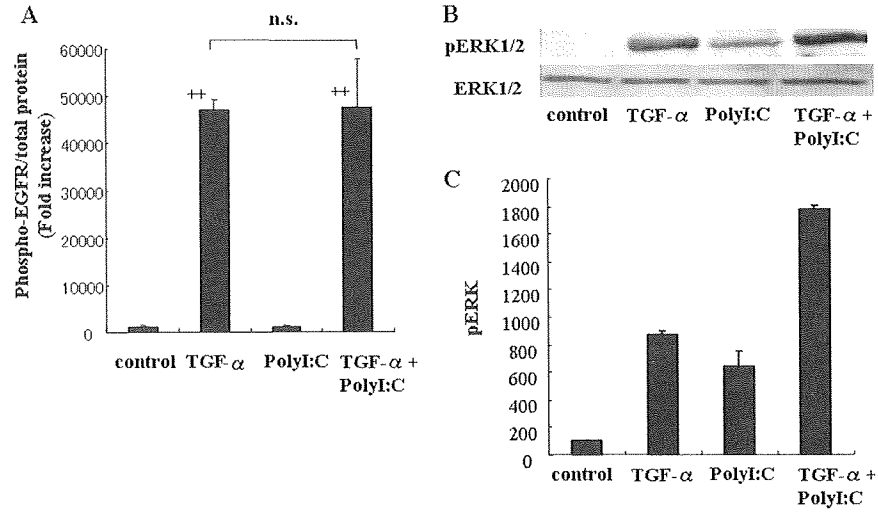

FIGURE 5. *A*, Relative phosphorylation of EGFR by poly(I:C) and TGF-α in NCI-H292 cells. Proteins extracted from samples collected were tested for the presence of phosphorylated EGFR by a Bio-Plex phosphoprotein assay kit using the Bio-Rad Luminex machine. The values plotted show the ratios of phosphorylated EGFR to total EGFR expressed as fold increase over control (n = 6). *B*, Phosphorylation of ERK1/2 by poly(I:C) (25 μg/ml) and TGF-α (4 ng/ml) in NCI-H292 cells assessed by performing Western blot analysis. *C*, Phospho-ERK was expressed as the fold increase in relative intensity (n = 3). Data are shown as means ± SD. ++, $p < 0.01$ compared with nonstimulated control cells.

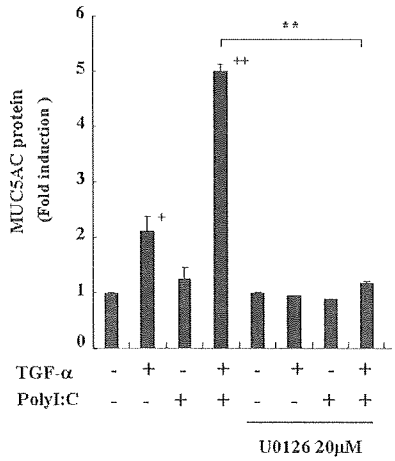

FIGURE 6. Effect of U0126 on poly(I:C)- and TGF-α-induced MUC5AC mucin production in NCI-H292 cells. Cells were preincubated with U0126 (a specific inhibitor of MEK1/2) at 20 μM (15, 16) for 1 h before adding poly(I:C) (75 μg/ml) and TGF-α (4 ng/ml), and cells were analyzed 24 h after stimulation ($n = 6$). Data are shown as means ± SD. +, $p < 0.05$ and ++, $p < 0.01$ compared with nonstimulated control cells. **, $p < 0.01$.

significantly induce MUC5AC mucin production in every dose, costimulation with TGF-α caused an increase in MUC5AC mucin production with regard to poly(I:C) in a dose-dependent manner (Fig. 2*A*). TGF-α alone induced a dose-dependent increase in MUC5AC mucin production, and poly(I:C) enhanced the effect of TGF-α (Fig. 2*B*). Subsequent studies were focused on the time course of MUC5AC mucin production. Costimulation with poly(I:C) (25 μg/ml) and TGF-α (4 ng/ml) caused a small increase in MUC5AC mucin production 12 h after stimulation, with maximal levels of MUC5AC at 24 h (Fig. 2*C*). These results may imply that poly(I:C) synergistically up-regulates MUC5AC mucin production induced by TGF-α.

Poly(I:C) synergistically enhances MUC5AC mRNA expression induced by TGF-α

To determine whether induction of MUC5AC mucin protein induced by poly(I:C) and TGF-α was a result of increased MUC5AC gene transcription, we investigated levels of MUC5AC mRNA, determined by real-time quantitative RT-PCR in NCI-H292 and NHBE cells. TGF-α (4 ng/ml) alone caused little increase in MUC5AC mRNA expression in NCI-H292 cells and NHBE cells upon 24 h of stimulation (Fig. 3*A*). Poly(I:C) (25 μg/ml) alone induced a small but significant increase in MUC5AC mRNA expression in both NCI-H292 cells and NHBE cells, and poly(I:C) strongly potentiated the effect of TGF-α (Fig. 3*A*). A clear dose response was observed at 12 h following stimulation with both poly(I:C) (2.5–75 μg/ml) (Fig. 3*B*) and TGF-α (0.4–12 ng/ml) (data not shown). Costimulation with poly(I:C) and TGF-α caused a small increase in MUC5AC mRNA expression 6 h after stimulation, which continued to a peak at 12 h after stimulation (Fig. 3*C*).

Poly(I:C) and TGF-α cause synergistic trans*-activation of the MUC5AC promoter*

We next investigated whether the MUC5AC promoter was activated by poly(I:C) and TGF-α. After 8 h, TGF-α alone induced a small but significant activation of the full-length MUC5AC promoter construct (−1330) (Fig. 4). Poly(I:C) did not activate the full-length MUC5AC promoter construct (−1330), but poly(I:C) strongly enhanced the activation induced by TGF-α, with 6-fold induction over that in unstimulated transfected control cells ($p < 0.05$) (Fig. 4). This was observed when poly(I:C) was added 12 h before TGF-α stimulation (Fig. 4), but not when the two agents were added at the same time (data not shown). There was no difference in the level of activation of the short-length MUC5AC promoter construct (−63) among TGF-α, poly(I:C), and both stimulations (Fig. 4). These results indicate that the −1330 to −63 region contains the elements regulating induction of the MUC5AC promoter by poly(I:C) and TGF-α.

Transactivation of the MUC5AC promoter by poly(I:C) and TGF-α is mediated via an ERK signaling pathway

Since it was shown that induction of MUC5AC-specific mucin protein by poly(I:C) and TGF-α was a result of increased MUC5AC gene transcription, we next investigated the upstream signaling leading to activation of the promoter.

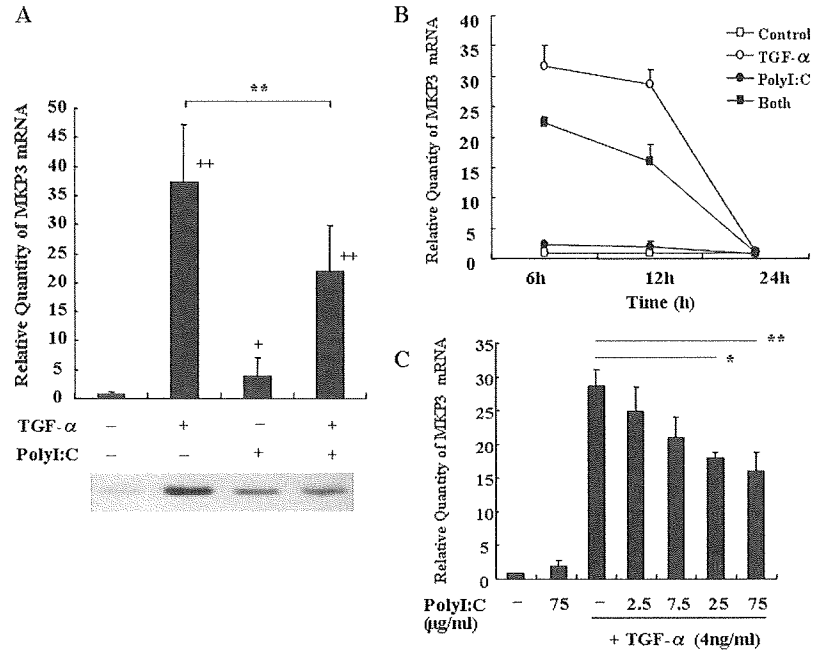

FIGURE 7. *A*, *Upper*, Effect of poly(I:C) (25 μg/ml) on TGF-α (4 ng/ml)-induced MKP3 mRNA expression in NCI-H292 cells ($n = 8$). *Lower*, To verify MKP3 expression in NCI-H292 cells, expression of MKP3 after stimulation with poly(I:C) (25 mg/ml) and TGF-α (4 ng/ml) was examined by standard RT-PCR. In brief, 25 μl of reaction mixture consisted of 1 μl cDNA, 1 pmol MKP3 primer sets, and 12.5 μl AmpliTaq Gold PCR Master mix (Applied Biosystems). PCR was performed by an initial denaturation step at 95°C for 5 min followed by 30 cycles with a denaturation step at 95°C for 30 s, an annealing step at 60°C for 30 s, and an extension step at 72°C for 30 s. *B*, Time course of induction of MKP3 mRNA expression by poly(I:C) (25 μg/ml) and TGF-α (4 ng/ml) in NCI-H292 cells ($n = 4$). *C*, Effect of the poly(I:C) concentration on TGF-α (4 ng/ml)-induced expression of MKP3 mRNA in NCI-H292 cells ($n = 4$). Data are shown as means ± SD. +, $p < 0.05$ and ++, $p < 0.01$ compared with nonstimulated control cells. *, $p < 0.05$ and **, $p < 0.01$.

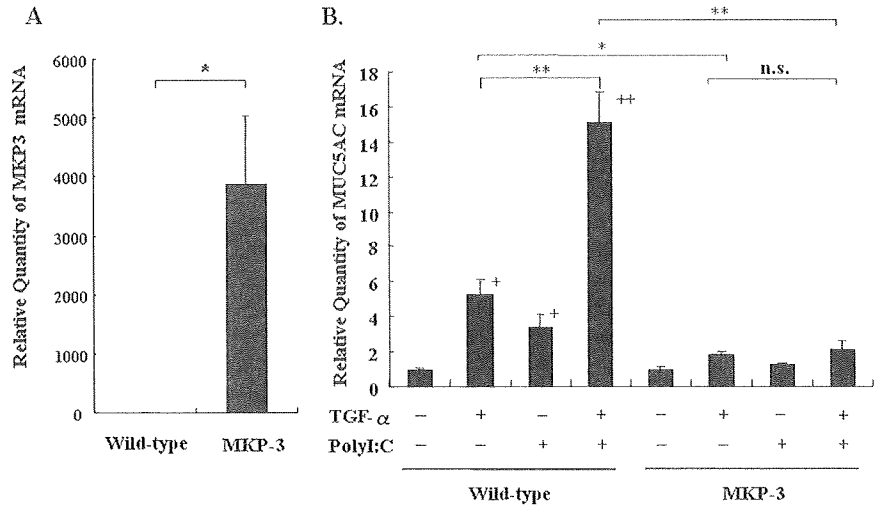

FIGURE 8. *A*, Effect of a MKP3 expression plasmid cloned into the pAcGFP1-C1 vector on MUC5AC mRNA expression in NCI-H292 cells. The level of MKP3 mRNA was enhanced significantly in cells transfected with the MKP3 expression plasmid. *B*, Enhanced expression of MUC5AC mRNA was noted in wild-type cells after 12 h of coincubation with TGF-α (4 ng/ml) and poly(I:C) (25 μg/ml), but it was completely abolished in cells transfected with the MKP3 expression vector ($n = 6$). Data are shown as means ± SD. +, $p < 0.05$ and ++, $p < 0.01$ compared with nonstimulated control cells. *, $p < 0.05$ and **, $p < 0.01$.

First, since TGF-α induces MUC5AC mucin production through the ligand-dependent *trans*-activation of EGFR in NCI-H292 cells (5), we examined the importance of EGFR activation for synergistic induction of MUC5AC mucin production by poly(I:C). We evaluated EGFR mRNA expression and phosphorylation of EGFR by RT-PCR and the Bio-Plex phosphoprotein assay, respectively. As a result, we found that poly(I:C) did not up-regulate EGFR mRNA expression upon 12 h of stimulation (data not shown) or increase the phosphorylation of EGFR (Fig. 5*A*).

Second, since previous studies have demonstrated that increased production of MUC5AC mucin protein after activation of the EGFR signaling pathway was exclusively MEK/ERK-dependent (17), we investigated the requirement of ERK. Western blot analysis revealed that poly(I:C) synergistically enhanced the phosphorylation of ERK by TGF-α stimulation (Fig. 5, *B* and *C*). This finding was compatible with the result of chemical inhibition by MEK1/2 inhibitor (U0126). U0126 inhibited the induction of MUC5AC protein production by poly(I:C) (75 μg/ml) and TGF-α (4 ng/ml) compared with absence of the inhibitor at 24 h after stimulation (Fig. 6). These data suggest that *trans*-activation of the MUC5AC promoter by poly(I:C) and TGF-α is mediated via an ERK signaling pathway.

Poly(I:C) inhibits TGF-α-induced MKP3 mRNA expression

Having demonstrated that the ERK-dependent signaling was required in MUC5AC induction, still unclear is the mechanism interacting between TLR3-dependent signaling stimulated by poly(I:C) and EGFR-dependent signaling stimulated by TGF-α. Since MKP3 is known to be a member of the phosphatase family that inactivates ERK1/2, we examined the effect of poly(I:C) on MKP3 mRNA expression. A real-time quantitative RT-PCR showed that expression of MKP3 mRNA was up-regulated upon 12 h of stimulation with TGF-α, and MKP3 mRNA up-regulation by TGF-α was inhibited by stimulation with poly(I:C) (Fig. 7*A*). Stimulation with TGF-α led to a moderate increase in MKP3 mRNA expression at 6 h, followed by a decrease at 24 h (Fig. 7*B*). Costimulation with poly(I:C) dose-dependently inhibited this up-regulation, and inhibition was seen from 6 h after stimulation (Fig. 7, *B* and *C*).

Effect of the MKP3 expression vector

To further demonstrate the role of MKP3 on MUC5AC mucin induction, we investigated the effect of MKP3 expression vector. MKP3 mRNA levels were significantly enhanced in cells transfected with the MKP3 expression plasmid cloned into the pAcGFP1-C1 vector when compared with wild-type cells (Fig. 8*A*). Enhanced expression of MUC5AC mRNA was noted in wild-type cells 12 h after coincubation with TGF-α (4 ng/ml) and poly(I:C) (25 μg/ml), but was completely abolished in cells transfected with the MKP3 expression vector (Fig. 8*B*). These data suggest that the inhibition of MKP3 mRNA expression by poly(I:C) leads to synergistic MUC5AC mucin induction.

Anti-IL-8 Ab does not inhibit poly(I:C)- and TGF-α-induced MUC5AC mRNA expression

Poly(I:C) is known to increase the expression of mRNA for various chemokines and cytokines (18, 19). In our preliminary study, we measured the cytokine and chemokine levels in the supernatant after stimulation with costimulation of TGF-α and poly(I:C) by using a Bio-Plex cytokine assay. In that study, only the IL-8 level was synergistically high due to costimulation of TGF-α and poly(I:C). Therefore, we chose IL-8, and to investigate the role of IL-8, NCI-H292 cells were preincubated with anti-IL-8 Ab 1 h before stimulation with poly(I:C) (75 μg/ml) and TGF-α (4 ng/ml). Anti-IL-8 Ab did not inhibit the increase in the expression of MUC5AC mRNA induced by 12 h of stimulation with poly(I:C) and TGF-α (Fig. 9).

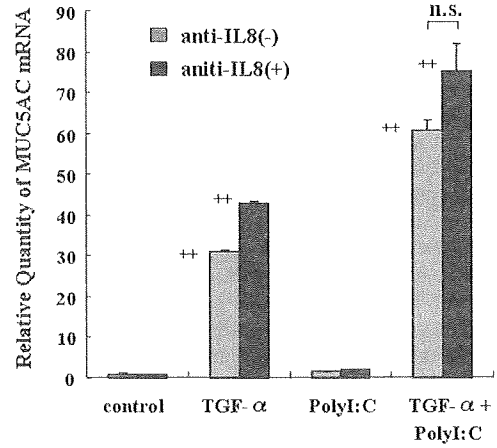

FIGURE 9. Effect of the anti-IL-8 Ab on poly(I:C) (75 μg/ml) and TGF-α (4 ng/ml)-induced MUC5AC mRNA expression in NCI-H292 cells ($n = 4$). Data are shown as means ± SD. ++, $p < 0.01$ compared with nonstimulated control cells.

Discussion

In this study, we found that poly(I:C) synergistically increased the production of MUC5AC induced by TGF-α in both NCI-H292 and NHBE cells. This increase was dependent on activation of the MUC5AC promoter, and the upstream signaling pathway was ERK-dependent. The most interesting finding of this study was that expression of MKP3, which is one of the negative regulators of MAPK, was up-regulated by TGF-α and this up-regulation was inhibited by poly(I:C), indicating that MKP3 has a central role in the synergistic induction of MUC5AC production by poly(I:C) and TGF-α.

Mucin hypersecretion and goblet cell hyperplasia are characteristic features of airway inflammatory diseases such as asthma (1, 2). Since hypersecretory diseases are associated with abnormal epithelial cell growth and differentiation, and epithelial damage leads to repair and remodeling (19, 20), both inflammatory mediators and growth factors may be involved in stimulating mucin production from goblet cells. It has been postulated that activation of the EGFR pathway is a common denominator in the induction of MUC5AC mucin, a major component of mucus in the airways. Takeyama et al. have shown that stimulation of EGFR by its ligands, EGF and TGF-α, causes MUC5AC production by airway epithelial cells both in vitro and in vivo (5), and this effect is potentiated by TNF-α (5). In the present study, we found that using AB-PAS staining, ELISA, and RT-PCR, poly(I:C) synergistically amplified the induction of MUC5AC mucin induced by TGF-α at both the mRNA and protein levels in NCI-H292 cells.

In NHBE cells, MUC5AC mRNA expression was much lower than that in NCI-H292 cells, but poly(I:C) still synergistically amplified the expression of MUC5AC mRNA induced by TGF-α, indicating that synergic induction of MUC5AC by poly(I:C) and TGF-α may be generalizable to normal human epithelial cells. The lower expression of MUC5AC mRNA may be explained by not using an air-liquid interface in culturing NHBE cells. Indeed, studies done in air-liquid interface or monolayers would provide us important results. However, previous studies have demonstrated that both NCI-H292 and NHBE cells share key components of the signaling pathways upstream and downstream of EGFR responsible for mucin production (21), suggesting that NCI-H292 cells are a valid model of mucin production in normal cells. Therefore, our further studies investigating the mechanisms of the signaling pathway were done in NCI-H292 cells.

In the present study, we found that synergistic induction of MUC5AC mucin production by poly(I:C) and TGF-α was dependent on activation of the MUC5AC promoter within the proximal $-1330/-63$ region. Additionally, we investigated upstream signaling by using an inhibitor and Western blot analysis, and we found that the process was ERK-dependent. Our data are in agreement with findings reported by Hewson and coworkers, showing that increased production of MUC5AC mucin protein after activation of the EGFR signaling pathway was exclusively MEK/ERK-dependent (17). Furthermore, we found that poly(I:C) synergistically enhanced the phosphorylation of ERK induced by TGF-α. Therefore, we concluded that *trans*-activation of the MUC5AC promoter by poly(I:C) and TGF-α occurs exclusively via an ERK signaling pathway.

Receptor regulation has an important role in controlling the actions of several mediators. Yamamoto et al. demonstrated that IL-4-induced production of eotaxin-3 in airway epithelium was enhanced due to up-regulation of the IL-4 receptor by IFN-γ (22). In the present study, to determine whether the synergistic effect of poly(I:C) was due to up-regulation of the EGFR, we evaluated EGFR mRNA expression and EGFR phosphorylation. However, up-regulation of EGFR mRNA expression and the phosphorylation of this receptor by stimulation with poly(I:C) were not observed.

Since we had found that ERK was required for the synergistic effect of poly(I:C) on MUC5AC production induced by TGF-α, we proceeded to investigate this further by evaluating the role of MKP3, which is a member of the phosphatase family that inactivates ERK1/2. MKP3 is predominantly localized in the cytoplasm and has a highly specific role in the dephosphorylation and inactivation of ERK1/2 (23–26). MKP3 is an immediate early gene and is transcriptionally up-regulated after ERK2 activation (27, 28). Our present finding that MKP3 mRNA expression was 37-fold higher following stimulation with TGF-α is in agreement with previous reports that MKP3 is up-regulated after activation of the ERK2 pathway (27–29). Additionally, we found that this up-regulation was inhibited by stimulation with poly(I:C), and that overexpression of MKP3 completely abolished the increase in expression of MUC5AC mRNA. These data indicate that when NCI-H292 cells are stimulated by TGF-α alone, MUC5AC protein production remains under autoregulation to a certain extent by negative feedback via MKP3. However, when additional stimulation with poly(I:C) is added, MKP3 mRNA expression is partially down-regulated. This leads to synergistic activation of ERK, synergistic *trans*-activation of the MUC5AC promoter, and finally to synergistic production of MUC5AC protein.

Posttranscriptional events are also important in regulation of gene expression. A detailed examination of the time course of MUC5AC mRNA expression revealed that it was maximal at 12 h and decreased at 24 h after treatment with TGF-α alone. In contrast, costimulation with poly(I:C) and TGF-α caused a significant time-dependent increase in MUC5AC mRNA expression for up to 24 h. Furthermore, analysis of mRNA stability by real-time quantitative RT-PCR demonstrated that poly(I:C) did not alter the stability of MUC5AC mRNA (data not shown). Accordingly, the additional stimulation with poly(I:C) significantly increased and prolonged the induction of MUC5AC mRNA expression induced by TGF-α without affecting the rate of MUC5AC mRNA degradation.

Poly(I:C) is known to increase the expression of mRNA for various chemokines (IP-10, RANTES, LARC, MIP1α, IL-8, GRO-α, and ENA-78) and cytokines (IL-1β, GM-CSF, and IL-6), as well as the cell adhesion molecule ICAM-1 (18, 19). To determine whether IL-8 has an important role in the synergistic effect of poly(I:C) and TGF-α on MUC5AC production, we investigated the potential role of IL-8 by preincubation with an anti-IL-8 Ab in the cells. The anti-IL-8 Ab did not inhibit MUC5AC mRNA expression, indicating that IL-8 has no role in the process. This finding was consistent with a previous report showing that IL-8 alone had no effect on MUC5AC protein production in NCI-H292 cells (30).

Also, the role of IFN may be an important point particularly in the context of poly(I:C) and asthma. We have not done studies directly on IFN-α and IFN-β. However, to further investigate whether extracellular factors (such as chemokines and cytokines) released by poly(I:C) stimulation up-regulated TGF-α-induced MUC5AC production, we changed the culture medium at 12 h after poly(I:C) stimulation and then stimulated the cells with TGF-α. Although the extracellular factors had been removed, it did not alter the synergic expression of MUC5AC mRNA (data not shown), suggesting that extracellular factors including IFN-α and IFN-β released by poly(I:C) may not contribute to the enhanced MUC5AC expression.

In conclusion, poly(I:C) synergistically increases the production of MUC5AC induced by TGF-α in airway epithelial cells, due to inhibition of MKP3 expression. Studies completed with viruses,

especially rhinovirus and also inactivated viruses, would provide us with important perspectives. Further studies will be needed to analyze the interaction between viruses and TGF-α. Viral respiratory tract infections are the most common triggers for the exacerbation of asthma (31, 32), and mucin overproduction is one of the mechanisms involved. The present findings may help to explain the excessive production of mucus in asthmatic patients with viral infection. Mucus plugging of the airways is a feature of fatal asthma in both adults and children (33, 34). At present, there are no effective therapies to relieve the symptoms induced by hypersecretion of mucus due to viral infection in asthmatic patients. Our findings may provide a mechanism to explain mucin overproduction and a potential strategy for therapy.

Acknowledgments

We thank Tomoko Endo and Chinori Iijima for their excellent technical assistance.

Disclosures

The authors have no financial conflicts of interest.

References

1. Ordonez, C. L., R. Khashayar, H. H. Wong, R. Ferrando, R. Wu, D. M. Hyde, J. A. Hotchkiss, Y. Zhang, A. Novikov, G. Dolganov, and J. V. Fahy. 2001. Mild and moderate asthma is associated with airway goblet cell hyperplasia and abnormalities in mucin gene expression. *Am. J. Respir. Crit. Care Med.* 163: 517–523.
2. Aikawa, T., S. Shimura, H. Sasaki, M. Ebina, and T. Takishima. 1992. Marked goblet cell hyperplasia with mucus accumulation in the airways of patients who died of severe acute asthma attack. *Chest* 101: 916–921.
3. Rogers, D. F. 2004. Airway mucus hypersecretion in asthma: an undervalued pathology? *Curr. Opin. Pharmacol.* 4: 241–250.
4. Hovenberg, H. W., J. R. Davies, and L. Carlstedt. 1996. Different mucins are produced by the surface epithelium and the submucosa in human trachea: identification of MUC5AC as a major mucin from the goblet cells. *Biochem. J.* 318: 319–324.
5. Takeyama, K., K. Dabbagh, H. M. Lee, C. Agustí, J. A. Lausier, I. F. Ueki, K. M. Grattan, and J. A. Nadel. 1999. Epidermal growth factor system regulates mucin production in airways. *Proc. Natl. Acad. Sci. USA* 96: 3081–3086.
6. Takeyama, K., J. V. Fahy, and J. A. Nadel. 2001. Relationship of epidermal growth factor receptors to goblet cell production in human bronchi. *Am. J. Respir. Crit. Care Med.* 163: 511–516.
7. Amishima, M., M. Munakata, Y. Nasuharu, A. Sato, T. Takahashi, Y. Homma, and Y. Kawakami. 1998. Expression of epidermal growth factor and epidermal growth factor receptor immunoreactivity in the asthmatic human airway. *Am. J. Respir. Crit. Care Med.* 157: 1907–1912.
8. Flolkerts, G., W. Busse, F. Nukamp, R. Sorkness, and J. Gern. 1998. Virus-induced airway hyperresponsiveness and asthma. *Am. J. Respir. Crit. Care Med.* 157: 1708–1720.
9. Johnston, S. L., P. K. Pattemore, and G. Sanderson. 1996. The relationship between upper respiratory infections and hospital admissions for asthma: a time-trend analysis. *Am. J. Respir. Crit. Care Med.* 154: 654–660.
10. Teichtahl, H., N. Buckmaster, and E. Pertnikovs. 1997. The incidence of respiratory tract infection in adults requiring hospitalization for asthma. *Chest* 112: 591–596.
11. Alexopulou, A., A. C. Holt, R. Medzhitov, and R. A. Flavell. 2001. Recognition of double-stranded RNA and activation of NF-κB by Toll-like receptor 3. *Nature* 413: 732–738.
12. Ieki, K., S. Matsukura, F. Kokubu, T. Kimura, H. Kuga, M. Kawaguchi, M. Odaka, S. Suzuki, S. Watanabe, H. Takeuchi, et al. 2004. Double-stranded RNA activates RANTES gene transcription through co-operation of nuclear factor-κB and interferon regulatory factors in human airway epithelial cells. *Clin. Exp. Allergy* 34: 745–752.
13. Deshmukh, H. S., L. M. Case, S. C. Wesselkamper, M. T. Borchers, L. D. Martin, H. G. Shertzer, J. A. Nadel, and G. D. Leikauf. 2005. Metalloproteinases mediate mucin 5AC expression by epidermal growth factor receptor activation. *Am. J. Respir. Crit. Care Med.* 171: 305–314.
14. Dziadziuszko, R., S. E. Witta, F. Cappuzzo, S. Park, K. Tanaka, P. V. Danenberg, A. E. Barón, L. Crino, W. A. Franklin, P. A. Bunn, et al. 2006. Epidermal growth factor receptor messenger RNA expression, gene dosage, and gefitinib sensitivity in non-small cell lung cancer. *Clin. Cancer Res.* 12: 3078–3084.
15. Park, C., S. Lee, I. Cho, H. K. Lee, D. Kim, S. Choi, S. B. Oh, K. Park, J. S. Kim, and S. J. Lee. 2006. TLR3-mediated signal induces proinflammatory cytokine and chemokine gene expression in astrocytes: differential signaling mechanisms of TLR3-induced IP-10 and IL-8 gene expression. *Glia* 53: 248–256.
16. Favata, M. F., K. Y. Horiuchi, E. J. Manos, J. A. Daulerio, D. A. Stradley, W. S. Feeser, D. E. Van Dyk, W. J. Pitts, R. A. Earl, F. Hobbs, et al. 1998. Identification of a novel inhibitor of mitogen-activated protein kinase kinase. *J. Biol. Chem.* 273: 18623–18632.
17. Hewson, C. A., M. R. Edbrooke, and S. L. Johnston. 2004. PMA induces the MUC5AC respiratory mucin in human bronchial epithelial cells via PKC, EGF/TGF-α, Ras/Raf, MEK, ERK and Sp1-dependent mechanisms. *J. Mol. Biol.* 344: 683–695.
18. Matsukura, S., F. Kokubu, M. Kurokawa, M. Kawaguchi, K. Ieki, M. Kuga, M. Odaka, S. Suzuki, S. Watanabe, H. Takeuchi, et al. 2006. Synthetic double-stranded RNA induces multiple genes related to inflammation through Toll-like receptor 3 depending on NF-κB and/or IRF-3 in airway epithelial cells. *Clin. Exp. Allergy* 36: 1049–1062.
19. Guillot, L., R. L. Goffic, S. Bloch, N. Escriou, S. Akira, M. Chignard, M. Chignard, and S.-T. Mustapha. 2005. Involvement of Toll-like receptor 3 in the immune response of lung epithelial cells to double-stranded RNA and influenza A virus. *J. Biol. Chem.* 280: 5571–5580.
20. Davies, D. E., R. Polosa, S. M. Puddicombe, A. Richter, and S. T. Holgate. 1999. The epidermal growth factor receptor and its ligand family: their potential role in repair and remodeling in asthma. *Allergy* 54: 771–783.
21. Shao, M. X., and J. A. Nadel. 2005. Dual oxidase 1-dependent MUC5AC mucin expression in cultured human airway epithelial cells. *Proc. Natl. Acad. Sci. USA* 102: 767–772.
22. Yamamoto, S., I. Kobayashi, K. Tsuji, N. Nishi, E. Muro, M. Miyazaki, M. Zaitsu, S. Inada, T. Ichimaru, and Y. Hamasaki. 2004. Upregulation of interleukin-4 receptor by interferon-γ: enhanced interleukin-4-induced eotaxin-3 production in airway epithelium. *Am. J. Respir. Cell Mol. Biol.* 31: 456–462.
23. Muda, M., A. Theodosiou, N. Rodrigues, U. Boschert, M. Camps, C. Gillieron, K. Davies, A. Ashworth, and S. Arkinstall. 1996. The dual specificity phosphatase M3/6 and MKP-3 are highly selective for inactivation of distinct mitogen-activated protein kinases. *J. Biol. Chem.* 271: 27205–27208.
24. Muda, M., U. Boschert, R. Dickinson, J. C. Martinou, I. Martinou, M. Camps, W. Schlegel, and S. Arkinstall. 1996. MKP-3, a novel cytosolic protein-tyrosine phosphatase that exemplifies a new class of mitogen-activated protein kinase phosphatase. *J. Biol. Chem.* 271: 4319–4326.
25. Zhou, B., L. Wu, K. Shen, J. Zhang, D. S. Lawrence, and Z. Y. Zhang. 2001. Multiple regions of MAP kinase phosphatase 3 are involved in its recognition and activation by ERK2. *J. Biol. Chem.* 276: 6506–6515.
26. Nichols, A., M. Camps, C. Gillieron, C. Chabert, A. Brunet, J. Wilsbachers, M. Cobb, J. Pouyssegur, J. P. Shaw, and S. Arkinstall. 2000. Substrate recognition domains within extracellular signal-regulated kinase mediate binding and catalytic activation of mitogen-activated protein kinase phosphatase-3. *J. Biol. Chem.* 275: 24613–24621.
27. Camps, M., C. Chabert, M. Muda, U. Boschert, C. Gillieron, and A. Arkinstall. 1998. Induction of the mitogen-activated protein kinase phosphatase MKP3 by nerve growth factor in differentiating PC12. *FEBS Lett.* 425: 271–276.
28. Camps, M., A. Nichols, C. Gillieron, B. Antonsson, M. Muda, C. Chabert, U. Boschert, and S. Arkinstall. 1998. Catalytic activation of the phosphatase MKP-3 by ERK2 mitogen-activated protein kinase. *Science* 280: 1262–1265.
29. Farooq, A., G. Chaturvedi, S. Mujtaba, O. Plotnikova, L. Zeng, C. Dhalluin, R. Ashton, and M. Zhou. 2001. Solution structure of ERK2 binding domain of MAPK phosphatase MKP-3: structural insights into MKP-3 activation by ERK2. *Mol. Cell.* 7: 387–399.
30. Takeyama, K., L. Dabbagh, J. J. Shim, T. Dao-Pick, I. Ueki, and J. A. Nadel. 2000. Oxidative stress causes mucin synthesis via transactivation of epidermal growth factor receptor: role of neutrophils. *J. Immunol.* 164: 1546–1552.
31. Schaller, M., C. M. Hogaboam, N. Kukacs, and S. L. Kunkel. 2006. Respiratory viral infections drive chemokine expression and exacerbate the asthmatic response. *J. Allergy Clin. Immunol.* 118: 295–302.
32. Johnston, S. L., P. K. Pattemore, G. Sanderson, S. Smith, F. Lampe, L. Josephs, P. Symington, S. O'Tool, S. H. Myint, D. A. Tyrrell, and S. T. Holgate. 1995. Community study of the role of viral infections in exacerbations of asthma in 9–11 year old children. *Br. Med. J.* 310: 1225–1228.
33. Sidebotham, H. J., and W. R. Roche. 2003. Asthma deaths; persistent and preventable mortality. *Histopathology* 43: 105–117.
34. Rogers, D. F. 2003. Pulmonary mucus: pediatric perspective. *Pediatr. Pulmonol.* 36: 178–188.

Risk Stratification in the Decision to Include Prednisolone With Intravenous Immunoglobulin in Primary Therapy of Kawasaki Disease

Tohru Kobayashi, MD, Yoshinari Inoue, MD,* Tetsuya Otani, MD,† Akihiro Morikawa, MD,* Tomio Kobayashi, MD,‡ Kazuo Takeuchi, MD, MPH,§ Tsutomu Saji, MD,¶ Tomoyoshi Sonobe, MD,‖ Shunichi Ogawa, MD,** Masaru Miura, MD,†† and Hirokazu Arakawa, MD**

Background: We reported previously that intravenous immunoglobulin (IVIG) plus prednisolone for initial therapy for Kawasaki disease (KD) prevented coronary artery abnormalities (CAA) more effectively than IVIG alone. However, questions remain as to whether PSL has potential benefit in all KD patients. The present study was designed to explore the possibility of stratified initial therapy including PSL in patients with and without a high predicted risk of being an IVIG nonresponder.

Methods: We retrospectively analyzed data from KD patients who received IVIG (n = 896) or IVIG + PSL (n = 110) by scoring the likely risk of being an IVIG nonresponder. We compared clinical and coronary outcomes between treatment-defined groups separately for high- and low-risk patients.

Results: Among low-risk patients (score 0–4), clinical and coronary outcomes were similar. Among high-risk patients (score 5 or more), incidences of treatment failure and coronary artery abnormalities until 1-month follow-up were more frequent in the IVIG than in the IVIG + PSL group. Sex- and score point-adjusted odds ratios for IVIG + PSL were 0.17 (95% confidence interval, 0.08–0.39) for treatment failure and 0.27 (95% confidence interval, 0.07–0.85) for coronary artery abnormalities A among high-risk patients.

Conclusions: IVIG + PSL treatment was associated with improving clinical and coronary outcomes in patients at high risk of being IVIG nonresponders.

Key Words: risk stratification, treatment failure, prednisolone, intravenous immunoglobulin, coronary artery abnormalities

(*Pediatr Infect Dis J* 2009;28: 498–502)

Kawasaki disease (KD) is an acute febrile illness of childhood characterized by clinical, biochemical, and histopathologic manifestations of systemic vasculitis.[1] Echocardiographic and cardiac angiographic data indicate that 20% to 25% of untreated KD patients develop coronary artery abnormalities (CAA).[2] Use of high-dose intravenous immunoglobulin (IVIG) together with aspirin is clearly effective in resolving inflammation in KD and reducing the occurrence of CAA.[3] However, about 10% to 20% of patients still have persistent or recurrent fever after completion of IVIG treatment, while CAA occur in about 10% of KD patients despite this therapy.[1] KD is presently considered to be the most common pediatric cause of acquired heart disease in developed countries.

Although corticosteroids are considered as a treatment option for various types of vasculitides, many physicians were uncomfortable with the use of corticosteroids in KD because of an early report,[4] showing a high incidence of CAA in a group that received a prolonged course of oral prednisolone (PSL) alone. Subsequent retrospective studies on effects of corticosteroids in KD, however, have shown either no ill effects or possible benefits.[5,6] Wooditch and Aronoff[7] concluded from a metaanalysis that inclusion of corticosteroids in aspirin-containing regimens for primary therapy for KD reduced the incidence of CAA. Recently, we reported a multicenter, prospective, randomized controlled trial demonstrating that primary therapy with IVIG plus PSL had a significant advantage over IVIG alone with respect to prevention of CAA and rapid resolution of inflammation.[8] Nonetheless, corticosteroid therapy may be associated with potential adverse reactions.[9–11] Additionally, a large fraction of IVIG responders, who account for 80% of KD patients, ultimately remain free of CAA.[12] Whether or not corticosteroids should be administered to all KD patients, therefore, is uncertain.

Recently, we developed a risk score that identified IVIG nonresponders in advance, with high sensitivity and specificity, based on 7 laboratory and demographic variables available before initiation of primary therapy.[13] This risk score could define 2 risk strata in patients with KD, indicating high- or low-risk for IVIG unresponsiveness. The risk score thus might enable us to identify KD patients who require more intensive primary therapy. We hypothesized that the addition of PSL to IVIG as primary therapy for KD patients would offer important therapeutic benefits to patients in this high-risk stratum. To explore the possibility of stratified primary therapy in KD patients, we retrospectively introduced risk stratification to identify the benefits of primary therapy, including PSL, in patients with and without a predicted high risk of IVIG unresponsiveness.

MATERIALS AND METHODS

Study Patients and Outline of Therapies

Data used for the present study were obtained from consecutive KD patients from August 2000 to August 2007 at 13 medical institutions in Gunma and Saitama prefectures in Japan. KD was diagnosed using the Japanese Diagnostic Guidelines for KD (fifth revised edition).[14] The first day of illness was defined as the first day of fever. Patients in the IVIG group received IVIG (1 g/kg/d

Accepted for publication November 13, 2008.
From the *Department of Pediatrics, Gunma University Graduate School of Medicine, Maebashi, Gunma, Japan; †Department of Health Policy, National Research Institute for Child Health and Development, Tokyo, Japan; ‡Department of Cardiology, Gunma Children's Medical Center, Gunma, Japan; §Faculty of Education, Saitama University, Saitama, Japan; ¶The First Department of Pediatrics, Toho University School of Medicine, Tokyo, Japan; ‖Department of Pediatrics, Japan Red Cross Medical Center, Tokyo, Japan; **Department of Pediatrics, Nippon Medical School, Tokyo, Japan; and ††Department of Cardiology, Tokyo Metropolitan Kiyose Children's Hospital, Tokyo, Japan.
Supported by Grants-in-Aid for Clinical Research for New Medicine from the Ministry of Health, Labor, and Welfare of Japan.
Address for correspondence: Tohru Kobayashi, MD, Department of Pediatrics, Gunma University Graduate School of Medicine, 3-39-22 Showa-machi, Maebashi, Gunma 371-8511, Japan. E-mail: torukoba@nifty.com.

ISSN: 0891-3668/09/2806-0498
DOI: 10.1097/INF.0b013e3181950b64

for 2 consecutive days or 2 g/kg/d for 1 day), whereas patients in the IVIG + PSL group received IVIG plus PSL (2 mg/kg/d, in 3 divided doses) given by intravenous injection until the fever resolved, and then orally until C-reactive protein (CRP) levels normalized (<0.5 mg/dL). After CRP normalized, doses of PSL were tapered over 15 days in 5-day steps (2 mg/kg/d for 5 days, 1 mg/kg/d for 5 days, and 0.5 mg/kg/d for 5 days). These methods of administration were based on our previous report.[5] Patients also received aspirin (30 mg/kg/d). The dose of aspirin was reduced to 5 mg/kg/d after normalization of CRP.

Clinical Outcomes and Stratification Using a Risk Score

The patient was considered afebrile when body temperature remained below 37.5°C for more than 24 hours. Nonresponse to initial treatment was defined as the patient having fever that persisted for more than 24 hours after completion of initial IVIG. Recurrence was defined as recrudescent fever associated with KD symptoms 24 hours after an afebrile period. These patients were defined as having treatment failure. CAA, detected by 2-dimensional echocardiography, were defined as present if the internal lumen diameter reached 3 mm in a child less than 5 years old, or at least 4 mm in a child aged 5 years or more; if the internal diameter of a segment was at least 1.5 times as large as that of an adjacent segment; or if the lumen was irregular. We stratified KD patients according to a risk scoring system developed to predict IVIG unresponsiveness. This risk score was based on a multiple logistic regression analysis, including 750 consecutive KD patients given IVIG. Seven variables were included in the risk score (Table 1). Point scores and cut-off values for each variable were as follows: 2 points each for sodium 133 mmol/L or less, 4 or less days of illness before initial treatment, aspartate aminotransferase (AST) 100 IU/L or more, percentage of white cells representing neutrophils at least 80%; and 1 point for platelet count 30.0 × 10^4/mm^3 or less, CRP at least 10 mg/dL, and age 12 months or less. If a laboratory test was performed twice or more before primary therapy, the highest value was chosen for % neutrophils, AST, and CRP, while the lowest value was chosen for platelet count and sodium. We considered KD patients as high risk when they had risk scores of 5 points or more.

Statistical Analysis

All analyses were carried out by means of the SPSS statistical package program (version 16.0J; SPSS Japan, Tokyo). Data were presented as mean ± SD for continuous variables or as a percentage for categorical variables. Patients who had missing values were excluded from this study. We compared clinical and coronary outcomes by dividing both treatment groups into high- and low-risk patients. Categorical data were compared between the IVIG group and the IVIG + PSL group using Fisher exact test. Two-sample t tests were used for analysis of normally distributed continuous variables, and the Mann-Whitney U test was used for continuous variables with a non-normal distribution. Normality was determined with the Kolmogorov-Smirnov algorithm. In high-risk patients, multiple logistic regression analysis was performed and odds ratios were adjusted for sex and score points. For all analyses, a 2-sided P value less than 0.05 was considered to indicate statistical significance.

TABLE 1. Risk Score for Prediction IVIG Unresponsiveness

Variable	Cut-Off Point	Score Point
AST	100 IU/L or more	2
Sodium	133 mmol/L or less	2
Illness days of initial treatment	4 or previous	2
Neutrophils	80% or more	2
CRP, (mg/dL)	10 mg/dL or more	1
Age in months	12 or less	1
Platelet counts	300,000 /mm^3 or less	1

RESULTS

Characteristics and Laboratory Findings of Patients

During the study period, 1123 KD patients were admitted and treated at our hospitals. Eight KD patients who presented with CAA at admission and 109 KD patients who had missing values were excluded from this study. Thus 1006 KD patients (IVIG group n = 896, IVIG + PSL group n = 110) were analyzed in this study. Of the 110 subjects in the IVIG + PSL group, 90 patients were participants in a previously reported randomized trial.[9] The other 20 patients were administered IVIG + PSL according to their pediatrician's selection except for one patient whose parents requested treatment with IVIG + PSL. Table 2 shows the baseline characteristics and laboratory findings of IVIG and IVIG + PSL groups. The IVIG + PSL group had significantly lower sodium, earlier illness days of initial treatment, and higher CRP and score points.

Univariate Analyses of Clinical Outcomes

Using the risk score, 298 patients (33.3%) in the IVIG group and 48 patients (43.6%) in the IVIG + PSL group were classified as high-risk patients (P = 0.034). In low-risk patients, clinical course and coronary outcomes did not show significant differences between IVIG and IVIG + PSL groups (Table 3). Only 5 patients in the IVIG group showed coronary dilation at 1 month, without giant coronary aneurysms exceeding 8-mm diameter. Table 4 summarizes clinical and coronary outcomes in high-risk patients. Treatment failure and nonresponse to initial treatment were less frequent in the IVIG + PSL group (20.8% and 8.3%, respectively) than in the IVIG group (51.7% and 47.3%, respectively; $P < 0.001$ both for comparison of treatment failure and for comparison of nonresponse to initial treatment). Similarly, the incidence of CAA before 1 month of treatment was significantly less in the IVIG + PSL group (3 patients, 6.3%; P = 0.037) than in the IVIG group (54 patients, 18.1%).

TABLE 2. Baseline Characteristics Both IVIG and IVIG + PSL Group

Variable	IVIG Group (n = 896)	IVIG + PSL Group (n = 110)	P
Male, n (%)	512 (57.1)	70 (63.6)	0.22
Age in months	30.3 ± 22.3	30.6 ± 23.9	0.87
Illness days of initial treatment	4.8 ± 1.4	4.5 ± 1.4	0.02
Past history of Kawasaki disease, n (%)	30 (3.3)	4 (3.6)	0.78
White blood cell counts, (×10^3/mm^3)	14.8 ± 5.0	14.9 ± 4.4	0.91
Neutrophils, (%)	68.8 ± 14.9	70.7 ± 15.0	0.20
Platelet counts, (×10^4/mm^3)	34.4 ± 10.7	36.1 ± 10.3	0.10
AST, (IU/L)	116 ± 222	127 ± 238	0.65
Sodium, (mmol/L)	134.6 ± 2.8	133.9 ± 3.0	0.01
CRP, (mg/dL)	8.6 ± 5.2	9.7 ± 5.2	0.05
Score points	3.5 ± 2.4	4.3 ± 2.5	0.002

TABLE 3. Clinical and Coronary Outcomes Among Low-Risk Patients

Variable	IVIG Group (n = 598)	IVIG + PSL Group (n = 62)	*P*
Treatment failure, n (%)	57 (9.5)	5 (8.1)	1.00
Nonresponse to initial treatment, n (%)	40 (6.7)	2 (3.2)	0.42
Relapse, n (%)	19 (3.2)	3 (4.8)	0.45
CAA until 1 mo, n (%)	14 (2.3)	0 (0.0)	0.38
CAA at 1 mo, n (%)	5 (0.8)	0 (0.0)	1.00

TABLE 4. Clinical and Coronary Outcomes Among High-Risk Patients

Variable	IVIG Group (n = 298)	IVIG + PSL Group (n = 48)	*P*
Treatment failure, n (%)	154 (51.7)	10 (20.8)	<0.001
Non-response to initial treatment, n (%)	141 (47.3)	4 (8.3)	<0.001
Relapse, n (%)	17 (5.7)	7 (14.6)	0.06
CAA until 1 mo, n (%)	54 (18.1)	3 (6.3)	0.04
CAA at 1 mo, n (%)	25 (8.4)	2 (4.2)	0.40

TABLE 5. Sex- and Risk Score Point-Adjusted Odds Ratios and 95% Confidence Intervals of Clinical and Coronary Outcomes Among High-Risk Patients

Variable	IVIG Group (n = 298)	IVIG + PSL Group (n = 48)	
		Adjusted OR	95% CI
Treatment failure	1.00 (reference)	0.18	(0.08–0.39)
Nonresponse to initial treatment	1.00 (reference)	0.07	(0.02–0.20)
Relapse	1.00 (reference)	2.75	(1.07–7.08)
CAA until 1 mo	1.00 (reference)	0.25	(0.07–0.85)
CAA at 1 mo	1.00 (reference)	0.41	(0.09–1.81)

OR indicate odds ratio.

Multivariate Analyses of Clinical Outcomes in High-Risk Group

Table 5 shows the sex- and risk score point-adjusted odds ratio of each of the end points. The IVIG + PSL group was at significantly lower risk of treatment failure (adjusted odds ratio 0.17; 95% confidence interval [CI], 0.08–0.39), nonresponse to initial treatment (adjusted odds ratio 0.07; 95% CI, 0.02–0.20), and CAA until 1 month of treatment (adjusted odds ratio 0.25; 95% CI, 0.07–0.85), despite having a significantly higher risk of relapse (adjusted odds ratio 2.75; 95% CI, 1.07–7.08).

DISCUSSION

The current study shows that risk-based stratification might guide decision making concerning initial treatment for KD. Among patients with high scores for risk of treatment failure with IVIG monotherapy, KD patients assigned to the IVIG + PSL treatment group were more likely to respond to therapy and avoid CAA. On the other hand, among patients with a low-risk of IVIG treatment failure, coronary and clinical outcomes were similar between the treatment-defined groups. These data suggest that primary therapy with a combination of IVIG and PSL might be a better therapeutic option than IVIG alone for this more severe form of KD. Patients with low risk of treatment failure might fare equally well with IVIG alone, thus limiting potential toxicities or adverse events due to steroid complications.

Stratification of primary therapy in KD patients was attempted in Japan in the 1990s. Harada[15] developed a risk score for prediction of coronary aneurysms for use when a child first presented with KD. Accordingly, at centers in Japan adopting this scoring system, IVIG was given to children fulfilling 4 of the following criteria: white blood cell count over 12000/mm^3; platelet count below 350000/mm^3; CRP exceeding 3+ by a semiquantitative analysis; hematocrit below 35%; albumin below 3.5 g/dL; age not greater than 12 months; and male gender. However, the influence of the Harada score in selecting KD patients who require IVIG has waned in Japan because IVIG is now given to almost all KD patients, as first-choice primary therapy. In addition, the American Heart Association and the American Academy of Pediatrics have recommended that all patients diagnosed with KD should be treated with IVIG, given the limited ability of scoring systems to predict CAA before initiation of IVIG.[16]

Pathologically, an affected coronary artery shows an influx of neutrophils in the early stage of lesion development (7–9 days after onset), followed by rapid transition to large mononuclear cells as well as lymphocytes (predominantly CD8$^+$ T cells) and IgA plasma cells.[17,18] Destruction of the internal elastic lamina followed by fibroblast proliferation occurs at this stage to form a coronary aneurysm. These findings underscore the importance of treating inflammation and vasculitis as soon as possible, before pathologic changes become irreversible. Recent clinical trials have focused on additional rescue therapy for KD patients who fail to respond to initial IVIG rather than primary therapy in KD. These rescue therapies have included corticosteroids,[19–21] tumor necrosis factor α blockade,[22] cyclosporine,[23] or plasma exchange.[24] Although these therapies were reported to bring about improvement in symptoms without significant worsening of adverse effects, no report concluded that these additional rescue therapies ultimately reduced the occurrence of CAA. Because IVIG nonresponders were mostly identified 24 to 48 hours after completion of the initial course of IVIG, rescue therapies generally were initiated 2 to 3 days after diagnosis of KD. Such a delay in administration of rescue therapies would permit initiation of CAA development. Because many studies have indicated that most KD patients with CAA are IVIG nonresponders,[12,13,25–26] the predictive identification of IVIG nonresponders permitting use of the additional intensive primary therapy, for IVIG plus corticosteroids should improve overall clinical and coronary outcomes.

Although we found addition of corticosteroids to IVIG primary therapy to benefit high-risk patients, the mechanism by which combining PSL with IVIG reduces the incidence of CAA in high-risk KD patients remains unclear. At this point, we suspect that rapid down-regulation of cytokine secretion by corticosteroid treatment might benefit high-risk patients because many investigators have concluded that various proinflammatory cytokines might take part in the pathogenesis of KD.[27,28] We previously reported that adding corticosteroids to IVIG when treating KD children rapidly ameliorated symptoms while reducing circulating cytokines, including interleukin IL-2, IL-6, IL-8, and IL-10.[29] Lin et al[30] reported that KD patients with CAA were found to have more abundant circulating pro-inflammatory cytokines, including IL-6, IL-8, and tumor necrosis factor α than patients with normal coronary arteries. Production of CRP occurs almost exclusively in hepatocytes as part of the acute-phase response upon stimulation by IL-6, tumor necrosis factor α, and IL-1β, produced at sites of inflammation. Although further studies are needed, these findings strongly support our inference that cytokine down-regulation con-